



## Synthesis, biological evaluation, and molecular docking analysis of novel linker-less benzamide based potent and selective HDAC3 inhibitors

Ganesh Routholla<sup>a,1</sup>, Sravani Pulya<sup>a,1</sup>, Tarun Patel<sup>a</sup>, Sk. Abdul Amin<sup>b</sup>, Nilanjan Adhikari<sup>b</sup>, Swati Biswas<sup>a</sup>, Tarun Jha<sup>b,\*</sup>, Balaram Ghosh<sup>a,\*</sup>

<sup>a</sup> Epigenetic Research Laboratory, Department of Pharmacy, BITS-Pilani, Hyderabad Campus, Shamirpet, Hyderabad 500078, India

<sup>b</sup> Natural Science Laboratory, Division of Medicinal and Pharmaceutical Chemistry, Department of Pharmaceutical Technology, P. O. Box 17020, Jadavpur University, Kolkata 700032, West Bengal, India

### ARTICLE INFO

#### Keywords:

Linker-less benzamides  
HDAC3 inhibitor  
Anticancer agent  
Histone acetylation  
Apoptotic cell death  
Cell cycle analysis

### ABSTRACT

A series of novel linker-less benzamides with different aryl and heteroaryl cap groups have been designed, synthesized, and screened as potent histone deacetylase (HDAC) inhibitors with promising anticancer activity. Two lead compounds **5e** and **5f** were found as potent and highly selective HDAC3 inhibitors over other Class-I HDACs and HDAC6. Compound **5e** bearing a 6-quinolinyl moiety as the cap group was found to be a highly potent HDAC3 inhibitor ( $IC_{50} = 560$  nM) and displayed 46-fold selectivity for HDAC3 over HDAC2, and 33-fold selectivity for HDAC3 over HDAC1. The synthesized compounds possess antiproliferative activities against different cancer cell lines and significantly less cytotoxic to normal cells. Molecular Docking studies of compounds **5e** and **5f** reveal a similar binding mode of interactions as **C1994** at the HDAC3 active site. These observations agreed with the *in vitro* HDAC3 inhibitory activities. Significant enhancement of the endogenous acetylation level on H3K9 and H4K12 was found when B16F10 cells were treated with compounds **5e** and **5f** in a dose-dependent manner. The compounds induced apoptotic cell death in Annexin-V/FITC-PI assay and caused cell cycle arrest at G2/M phase of cell cycle in B16F10 cells. These compounds may serve as potential HDAC3 inhibitory anticancer therapeutics.

### 1. Introduction

According to WHO, cancer is the second leading cause of death worldwide, claiming about 9.6 million deaths (approximately 1 in 6) in 2018 [1]. "Cancer is caused by the mutations in tumor suppressor genes and oncogenes due to epigenetic manipulations that lead to cell proliferation and differentiation" and this is considered the most acceptable hypothesis in cancer pathogenesis [2]. It is also well-established that genetic and epigenetic modifications contribute to the development of cancer [3]. Epigenetic modifications leading to structural changes in chromatin include DNA methylation, and post-translational modifications of histone proteins. Among the post-translational modifications, histone acetylation and deacetylation have been found to play a pivotal role in the regulation of expression of genes involved in cancer pathogenesis [4]. Histone acetyl transferases (HATs) and histone deacetylases (HDACs) are the two key enzymes involved in the regulation of gene expression through acetylation and deacetylation of histone proteins at

ε-amino group of lysine residues present in the N-terminal end of histone proteins. The imbalance between the activities of HATs and HDACs often results in aberrant gene expression leading to several epigenetic disorders [5]. Moreover, HDACs play a prominent role also in cancer cell proliferation, invasion, and metastasis [6]. It has also been reported that HDAC inhibitors are well-implicated in apoptosis or programmed cell death as well as cell cycle arrest [7–9], whereas abnormal HDAC expression lead to various cancers such as cancers of colon, breast, liver, lung, pancreas, prostate, along with melanoma, lymphoma, multiple-myeloma and leukaemia [10]. There are 18 different HDACs categorized into four classes according to their homology with yeast proteins, subcellular localization, and mechanism of action. Basically, Class I (HDAC1, 2, 3 and 8), Class II (IIa: HDAC4, 5, 7 and 9; IIb: HDAC6 and 10) and Class IV (HDAC 11) HDACs are Zn<sup>+2</sup>-dependent whereas Class III HDACs are NAD<sup>+</sup>-dependent also known as Sirtuins (SIRT 1–7) [6,11].

HDAC3 has garnered lot of attention due to its implication in various

\* Corresponding authors.

E-mail address: [balaram@hyderabad.bits-pilani.ac.in](mailto:balaram@hyderabad.bits-pilani.ac.in) (B. Ghosh).

<sup>1</sup> Authors have equal contribution.

life-threatening disease conditions namely cancers [9], cardiovascular diseases [12], memory and learning disorders [13,14], neurodegenerative diseases [15], diabetes [16] and rheumatoid arthritis [17]. Most importantly, HDAC3 has been validated and well-studied as a potential target for cancer therapy, due to its crucial role in transcriptional repression through hypoacetylation of histones in different cancers [18]. HDAC3 has been found to modulate various cancers such as colon cancer [19], breast cancer [20], multiple myeloma [21], melanoma [22], prostate cancer [23], gastric cancer [24] and leukemia [25], and selective HDAC3 inhibitors have been extensively studied in recent years for various applications [9,26]. However, still lot of work needs to be carried out to identify highly potent and selective HDAC3 inhibitors to combat such disease states with minimum off target side effects. HDAC3, a well-explored Class I HDAC, is structurally characterized by a unique C-terminal domain and it forms a stable complex with NCoR and SMRT for carrying out the deacetylase activity [27]. Several amino acid residues (such as Tyr198, Asp92, Phe199, Tyr107) at the active site of HDAC3 contribute to the substrate specificity over other Class I HDAC isoforms. Nevertheless, the interactions of Ins(1,4,5,6) $P_4$  and DAD with HDAC3 contribute to the activation of the enzyme [28,29]. The general pharmacophore model of HDAC active site includes a surface binding domain that interacts with the cap group, the hydrophobic channel that recruits the linker region, and the catalytic zinc binding domain where the  $Zn^{2+}$  ion interacts with the zinc binding group (ZBG) of the HDAC inhibitors (Fig. 1). There is also an internal cavity adjacent to the zinc binding domain in case of HDAC3 isoform that might contribute its substrate specificity [30].

Quite a few number of HDACis have been reported so far and they are widely studied in pre-clinical and clinical phases as anticancer agents [9]. Based on various ZBGs, different classes of HDACis have been reported such as hydroxamates, benzamides, short chain fatty acids, cyclic tetrapeptides, hydrazides and thiols [9]. Six HDACis have been clinically approved so far namely vorinostat, belinostat, panobinostat, romidepsin, chidamide and pracinostat for the treatment of different cancers such as cutaneous T-cell lymphoma, peripheral T-cell lymphoma, multiple myeloma and acute myeloid leukemia [31]. With the multiple side-effects and dose-limiting toxicities associated with these *pan*-HDACis, the need for developing novel isoform specific inhibitors has been realised urgently to overcome these limitations and to improve the potency and specificity towards individual HDAC isoforms.

The above mentioned clinically approved HDAC inhibitors belong to hydroxamate class except chidamide which is the only benzamide compound approved by Chinese FDA for the treatment of relapsed peripheral T-cell lymphoma [32]. Interestingly, several studies have been carried out and are still continuing on benzamide class of compounds to come up with selective HDAC inhibitors with minimum or no off target side effects [9]. Notably, the benzamide based class-I HDAC selective inhibitors such as entinostat (MS-275, 1) [33] and tacedinaline (CI994, 4) [35,36] and HDAC3 selective inhibitors, RGFP109 (2) [34], and BG45 (3) [21] have been studied extensively as promising anticancer agents (Fig. 2). Recently, several other benzamides designed with varying cap groups have been reported with enhanced HDAC3 selectivity and inhibition potential [9].

Benzamide has been established as a promising moiety responsible for chelating the  $Zn^{2+}$  ion for various HDACs and thereby responsible for potent inhibition along with selectivity towards specific HDACs

[13,18,37,38]. Since last 10 years, a number of research works have been carried out on this scaffold to design compounds reflecting potent HDAC3 inhibition along with selectivity over other HDACs [39,40,40–47]. Interestingly, these compounds also comprise the typical features as HDAC inhibitors, i.e., the cap group, the linker moiety and the ZBG. However, only a few group of researchers tried to design linker-less atypical selective HDAC3 inhibitors [20,47]. Minami et al. [21] first reported BG45, which is a linker-less benzamide based HDAC3 selective inhibitor, showed promising efficacy against multiple myeloma. Another series of linker-less HDAC3 selective compounds have been reported by McClure et al. [48]. They used benzofuran scaffold instead of pyrazine scaffold of BG45 to obtain potent and selective HDAC3 inhibitors. Our group has been actively working on the development of HDAC3 selective inhibitors with an emphasis on benzamides involving the structural modifications of the cap and linker region [18,49–53]. We, hereby, report a series of linker-less benzamide compounds with different cap groups derived from the basic pharmacophore scaffold of CI994 which has been studied most extensively in preclinical and clinical applications [35](Fig. 2). In-order to enhance the HDAC3 selectivity, modification of the cap region with different aromatic or heteroaromatic functions of the linker-less benzamides have been reported.

Herein, we report the synthesis schemes, HDAC3 isoform selectivity study and detailed biological characterization of the synthesized small molecule HDAC3 inhibitors.

## 2. Results

### 2.1. Chemistry

#### 2.1.1. Design and synthesis of novel benzamides

Keeping the benzamide scaffold intact as the ZBG, several aryl (such as phenyl, naphthyl) and heteroaryl (such as quinolinyl, indolyl, thienyl and pyrazinyl-aminophenyl) cap groups have been incorporated. Most of these benzamides (5a–5h) were synthesized as per Scheme 1 whereas compound 5i was synthesized following the Scheme 2.

As per Scheme 1, the aromatic or heteroaromatic carboxylic acids (3a–3h) were purchased commercially and were coupled with *tert*-butyl (2-aminophenyl) carbamate synthesized as per protocol reported previously [49]. Under the conditions, the acid-amine coupling reactions were done using EDCI as coupling agent to obtain (4a–4h) as the intermediates, which upon deprotection of carbamate group in acidic medium afforded the final compounds (5a–5h).

Considering the contribution of pyrazine scaffold to the enhanced HDAC3 selectivity as in the case of BG45, another molecule with aminophenyl as the cap group attached to the pyrazine scaffold at its 2nd position with the benzamide has been designed and synthesized. Scheme 2 describes the synthesis of compound 5i. There 6-chloro pyrazine-2-carboxylate (1i) was converted to methyl 6-(phenylamino) pyrazine-2-carboxylate (2i) using aniline in the presence of NMP as a solvent and DIPEA as a base. The 6-(phenylamino) pyrazine-2-carboxylic acid (3i) was obtained through alkaline hydrolysis of the carboxylate (2i). The acid 3i was coupled with *tert*-butyl (2-aminophenyl) carbamate synthesized as per our previous report [49]. Under the conditions, acid-amine coupling was conducted using EDCI as coupling agent to obtain (4i) as the intermediate, which upon deprotection of carbamate group in acidic medium resulted in the final compound 5i.

The structures of the designed and synthesized compounds along with their % yield and physicochemical properties are listed in Table 1. Physicochemical characterisations of the synthesized molecules were done using  $^1H$  NMR,  $^{13}C$  NMR, HRMS analysis and the spectral data is given in the supporting information section (Spectra S1 – S36).



Fig. 1. General pharmacophoric structure of HDAC inhibitors.

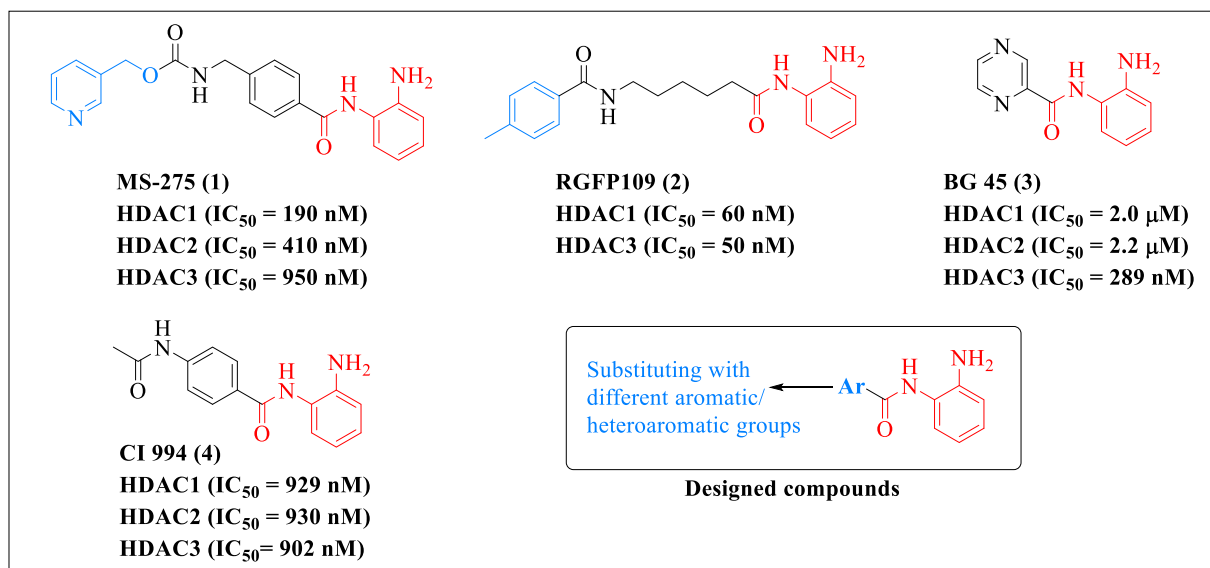
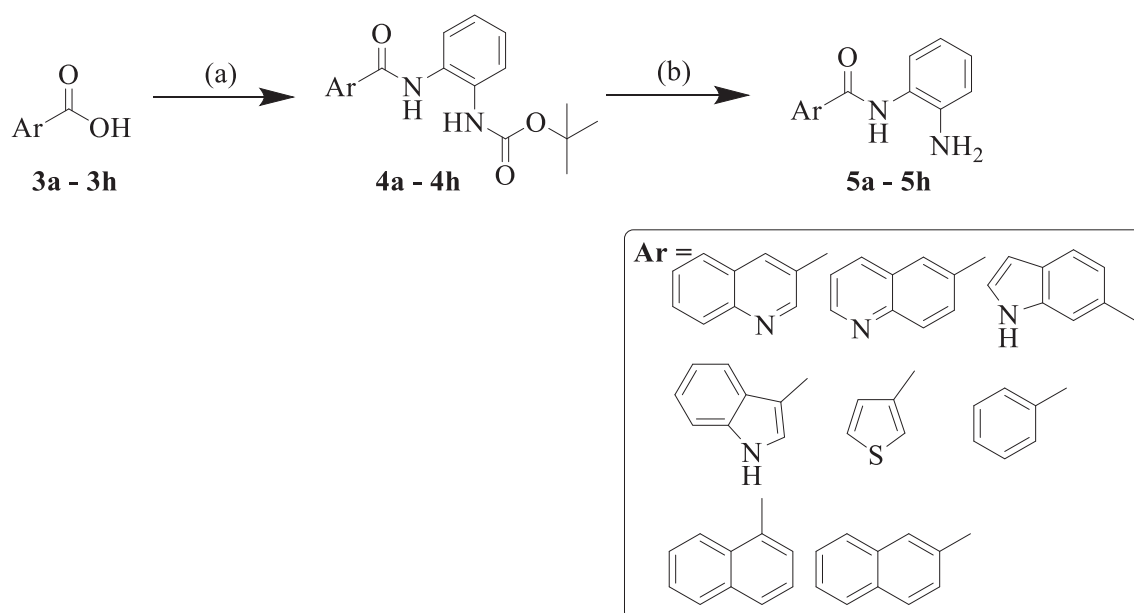


Fig. 2. Structures of benzamide derivatives and design of our new benzamides derivatives.



Scheme 1. Reagents and conditions: (a) *tert*-butyl 2-amino phenyl carbamate, EDC, DMAP, DCM:pyridine (1:1), RT (b) 4 M HCl in dioxane, 0 °C, 2 h.

## 2.2. Biological evaluation

### 2.2.1. Pan-HDAC and HDAC3 inhibition

All the synthesized compounds (**5a-5i**) were screened for enzyme inhibitory activity towards *pan*-HDAC (HeLa Nuclear extract) and recombinant human HDAC3 enzymes initially (supporting Figure S1 and S2). All the compounds exhibited effective % inhibition of pan HDAC activity at 10 μM compound concentration and effective % inhibition HDAC3 activity at 1 μM compound concentration are depicted in Table 2.

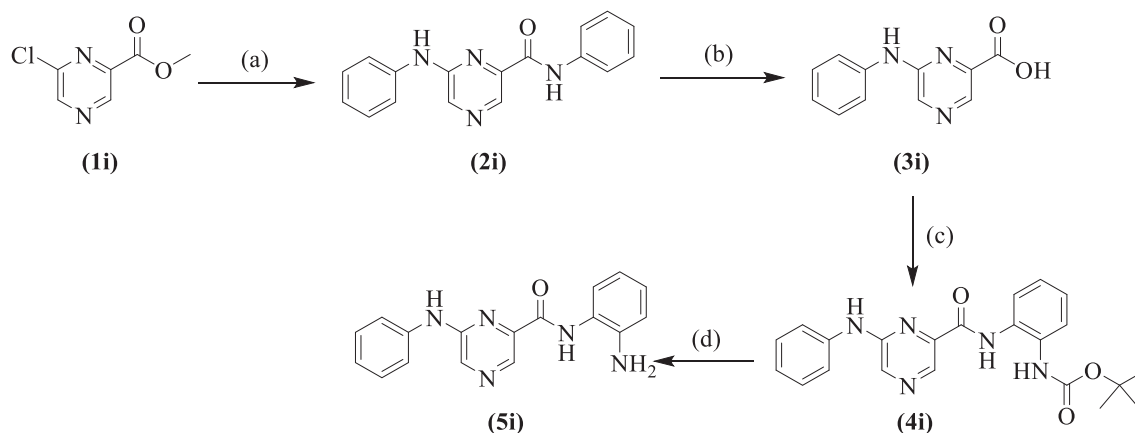
It was interesting to note that all these compounds (**5a-5i**) exhibited comparatively less *pan*-HDAC inhibitory activity compared to the reference molecule **CI994** and compound **5e** showed least pan HDAC inhibition in the series. However, in case of HDAC3 inhibition, compound **5e** (59%) was found to be most active and even better inhibitor than **CI994** (53.65%). Further, it can be inferred from the % inhibition values, that though **5a** exhibited considerable HDAC inhibitory activity

but the selectivity factor towards HDAC3 is less when compared to that of compound **5e** which is highly potent with 59% inhibition at 1 μM. It was noteworthy that the pyrazine scaffold containing benzamide compound, **5i** neither exhibited any significant *pan*-HDAC or HDAC3 inhibition when compared to other compounds in the series.

### 2.2.2. HDAC isoform inhibition

From the result of initial screening based on their inhibition potency, we have further selected compounds **5e** and **5f** for the determination of IC<sub>50</sub> values which will give more precise potency and selectivity towards HDAC3. The selected compounds **5e** and **5f** along with the standard reference **CI994** were subjected to their IC<sub>50</sub> determination towards HDAC1, HDAC2, HDAC3, HDAC6 and HDAC8 isoforms (Fig. 3, Table 3).

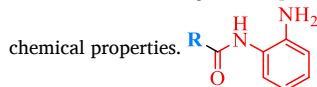
Compounds **5e** and **5f** displayed IC<sub>50</sub> values of 0.560 μM and 2.077 μM against HDAC3 respectively and that are the highest potency towards HDAC3 compared to that of other HDAC isoforms (Table 3). Interestingly, compound **5e** was found to be more effective towards



**Scheme 2.** Reagents and conditions: (a) Aniline, *N*-methyl 2-pyrrolidone (NMP), DIPEA, 160 °C, 20 h, reflux (b) NaOH, MeOH, H<sub>2</sub>O, 1 h (c) *tert*-butyl 2-amino phenyl carbamate, EDCI, DMAP, DCM: pyridine (1:1), RT (d) 4 M HCl in dioxane, 0 °C, 2 h.

**Table 1**

Structures of the designed compounds along with their % yield and physico-



Compound	R	% yield	HBD	HBA	Log P
5a		87.00	2	2	2.04
5b		70.00	2	2	3.03
5c		71.85	2	2	3.03
5d		55.00	2	3	1.87
5e		80.00	2	3	1.87
5f		70.00	3	3	1.58
5g		57.30	3	3	1.58
5h		86.00	2	2	1.96
5i		88.80	3	5	1.97

HDAC3 than even the reference molecule **CI994** ( $IC_{50} = 0.902 \mu M$ ). The  $IC_{50}$  determining dose response curves of the selected compounds **5e** and **5f** against different HDAC isoforms are shown in the Fig. 3. It was interesting to observe that the reference molecule **CI994** was nonselective towards HDAC3 over HDAC1 and HDAC2 (Table 3). However, Compound **5e** bearing a 6-quinolonyl moiety as the cap group was found to be highly potent HDAC3 inhibitor ( $IC_{50} = 560$  nM) and displayed 46-fold selectivity for HDAC3 over HDAC2 and 33-fold selectivity for HDAC3 over HDAC1. Interestingly, there was about 4-fold reduction of HDAC3 inhibition ( $IC_{50} = 2.077 \mu M$ ) compared to the former one when the quinolone cap group of **5e** was replaced by 6-indolyl cap in compound **5f** but still retained a minimum of 5-fold HDAC3 selectivity over

**Table 2**

The % inhibition values of enzymatic activity by the synthesized compounds as well as the reference molecule **CI994** against Hela nuclear extract (*Pan*-HDAC activity) and recombinant HDAC3 enzymes. Data represents mean  $\pm$  SD (n = 2).

Compound	<i>Pan</i> -HDAC % Inhibition (at 10 $\mu M$ )	HDAC3 % Inhibition (at 1 $\mu M$ )
5a	38.46 $\pm$ 1.68	19.35 $\pm$ 1.17
5b	15.11 $\pm$ 2.27	22.74 $\pm$ 0.24
5c	32.88 $\pm$ 0.95	33.06 $\pm$ 1.88
5d	22.40 $\pm$ 3.12	21.83 $\pm$ 0.83
5e	12.9 $\pm$ 0.85	59 $\pm$ 0.46
5f	31.67 $\pm$ 1.07	21.13 $\pm$ 2.67
5g	22.42 $\pm$ 4.15	21.38 $\pm$ 2.75
5h	27.86 $\pm$ 0.56	34.45 $\pm$ 2.81
5i	17.78 $\pm$ 0.61	7.93 $\pm$ 1.25
CI994	53.8 $\pm$ 0.91	53.65 $\pm$ 1.21

other HDAC isoforms tested. Conclusively, compound **5e** is the most potent HDAC3 inhibitor and has been considered to be a lead molecule from this series with excellent selectivity towards HDAC3 while compared to other compounds including reference compound **CI994**.

### 2.2.3. Anti-proliferative assay against cancer cell lines

All these final compounds (**5a-5i**) along with the reference molecule **CI994** were evaluated for their antiproliferative activity against human triple-negative breast cancer cell line (MDA-MB-231), mouse breast cancer cell line (4 T1) and murine melanoma cancer cell line (B16F10) by MTT assay (Fig. 4A-4C).

Initially, all the synthesized compounds were tested at two different concentrations (100  $\mu M$  and 10  $\mu M$ ) in duplicate taking **CI994** as reference molecule (supporting Figure S3 – S6) to have an idea about the cell growth inhibition potential of the compounds. Based on the results from initial two dose screen the  $IC_{50}$  values of all the compounds were determined with a wider range of compound concentrations. The compounds displayed effective anticancer efficacies against the tested cancer cell lines with good selectivity for cancer cell lines over normal cell lines (Table 4).

The data signifies that the antiproliferative activity of all the compounds was comparable to the reference **CI994** in all the cancer cell lines tested. In fact, some of these compounds (Compounds **5a**, **5b**, **5d** and **5i**) resulted in more or less similar anticancer efficacy to **CI994** (Table 4). Regarding the cytotoxicity against mouse breast cancer cell line 4T1, only compounds **5b** and **5f** exhibited better cytotoxicity ( $IC_{50}$  of 13.25 and 14.30  $\mu M$ , respectively) than **CI994** ( $IC_{50} = 16.74 \mu M$ ). However, in case of cytotoxicity against murine melanoma cancer cell line B16F10, several compounds (compounds **5a**, **5b**, **5c**, **5i** and **5h**) also yielded better cytotoxicity compared to **CI994** ( $IC_{50} = 14.34 \mu M$ ) (Table 4). The

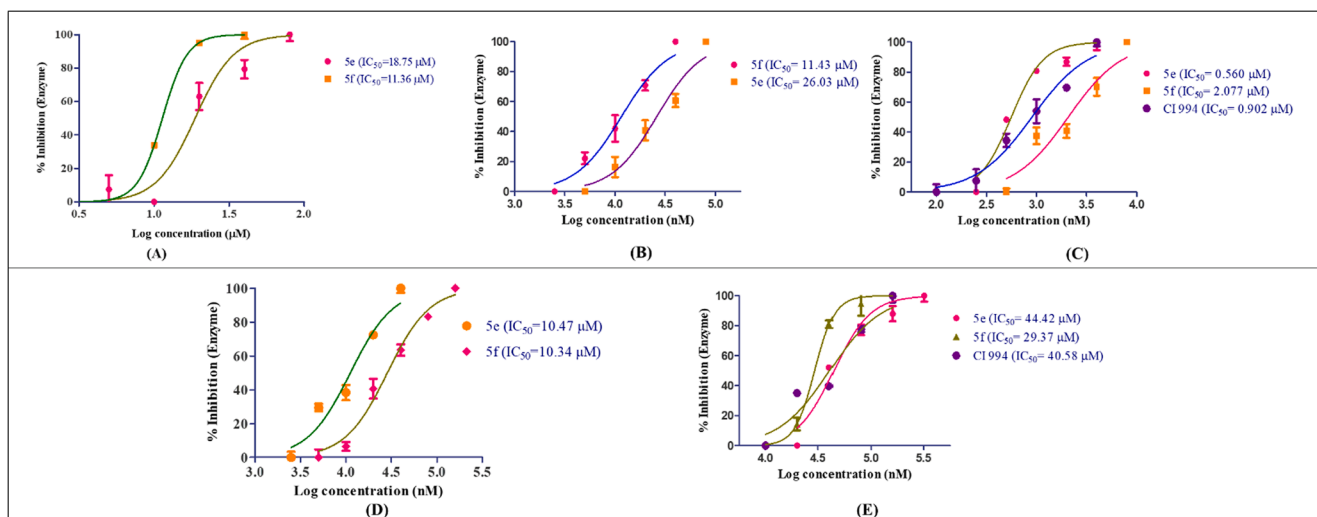


**Fig. 3.** The dose response curve for  $IC_{50}$  determination of compounds **5e** and **5f** using **CI994** as positive control. (A) Using kit based human recombinant HDAC1 enzyme assay. (B) Using kit based human recombinant HDAC2 enzyme assay. (C) Using kit based human recombinant HDAC3/NCOR1 enzyme assay. (D) Using kit based human recombinant HDAC8 enzyme assay. (E) Using kit based human recombinant HDAC6 enzyme assay [ $IC_{50}$  determinations were carried out in the concentration range of 0.061 – 80  $\mu$ M of the compounds in duplicate as per the protocol given in the HDAC enzyme assay kits purchased from bio nova. The  $IC_{50}$  values of these compounds were determined using nonlinear regression analysis method using Graph Pad Prism 5. Data represent mean  $\pm$  SD (n = 2)].

**Table 3**

The  $IC_{50}$  values of compounds **5e** and **5f** using **CI994** as positive control on human recombinant HDAC1, 2, 3, 8 and 6 isoforms and their HDAC3 selectivity profile. Data represent mean  $\pm$  SD (n = 2).

Cpd	$IC_{50}$ ( $\mu$ M)					Selectivity for HDAC3 over other HDACs			
	HDAC1	HDAC2	HDAC3	HDAC8	HDAC6	HDAC1/3	HDAC2/3	HDAC8/3	HDAC6/3
CI994	0.929 $\pm$ 0.06	0.93 $\pm$ 0.09	0.902 $\pm$ 0.14	19.57 $\pm$ 2.1	40.58 $\pm$ 3.2	1.03	1.03	21.7	44.99
5e	18.75 $\pm$ 1.98	26.03 $\pm$ 1.2	0.560 $\pm$ 0.11	10.47 $\pm$ 0.71	44.42 $\pm$ 2.31	33.48	46.48	18.7	79.32
5f	11.36 $\pm$ 0.87	11.43 $\pm$ 0.89	2.077 $\pm$ 0.69	10.34 $\pm$ 1.01	29.37 $\pm$ 1.32	5.47	5.5	4.98	14.14

$\beta$ -naphthyl derivative (compound **5c**) and pyrazine derivative (compound **5i**) resulted in potent cytotoxicity in B16F10 cell line with an  $IC_{50}$  of 9.26 and 9.39  $\mu$ M, respectively (Table 4). Again, in case of cytotoxicity in breast cancer cell line, MDA-MB-231, compounds **5b**, **5c**, **5d** and **5g** displayed better efficacy than **CI994** ( $IC_{50}$  = 15.14  $\mu$ M) (Table 4). Among these molecules, compound **5c** was the most cytotoxic one ( $IC_{50}$  = 7.92  $\mu$ M). Interestingly, compound **5b** ( $IC_{50}$  values 11.81  $\mu$ M in MDA-MB-231 and 12.77  $\mu$ M in B16F10 cells) and compound **5c** ( $IC_{50}$  values 7.92  $\mu$ M in MDA-MB-231 and 9.26  $\mu$ M in B16F10 cells) exhibited higher  $IC_{50}$  values than **CI994** ( $IC_{50}$  values 15.14  $\mu$ M in MDA-MB-231 and 14.34  $\mu$ M in B16F10 cells) but showed least enzyme inhibitory potency. Though compounds **5e** and **5f** exhibited higher HDAC3 inhibitory potency and selectivity than remaining compounds, they were found to be moderately active against MDA-MB-231, 4T1 and B16F10 cells. All the remaining compounds exhibited comparable  $IC_{50}$  values against MDA-MB-231 cells and B16F10 cells (Fig. 4A and 4C). However, in case of 4T1 cells, the  $IC_{50}$  values for the remaining compounds were found to be higher than that of the reference compound **CI994** (Fig. 4B).

#### 2.2.4. In vitro cytotoxicity against normal HEK293 cell lines

Furthermore, the cellular toxicity of all the compounds were tested against normal human embryonic kidney (HEK293) cell line for their  $IC_{50}$  determination (Fig. 4D). The compounds were found to be less cytotoxic towards HEK293. Interestingly, compounds **5e** and **5f** with the  $IC_{50}$  values of 1.08 mM and 753.3  $\mu$ M were found to be significantly less toxic than all the other compounds tested and consequently possessed higher selectivity towards all the cancer cell lines over normal HEK293 cells (Table 4).

#### 2.2.5. Induction of histone hyper-acetylation in B16F10 cells: Western blot analysis

The cellular HDAC inhibitory activity of compounds **5e** and **5f** along with reference molecule **CI994** was carried out to find the compounds ability to induce histone acetylation in B16F10 cells by western blot analysis. The histone acetylation level was measured in a dose-dependent manner with compounds **5e** and **5f** on H3K9 and H4K12 as endogenous histone substrates. Treatment of compounds **5e**, **5f** and **CI994** was carried out for 12 h at concentrations of 5  $\mu$ M and 20  $\mu$ M that induced significant acetylation of H3K9 and H4K12 in a dose-dependent manner (Fig. 5 and Fig. 6). The upregulation of histone acetylation was in consistent with the *in vitro* HDAC inhibitory activity and also with the cellular antiproliferative activity.

#### 2.2.6. Nuclear staining assay

Further to study the phenotype effect of compounds in cells, nuclear staining assay was performed using DAPI and AO as staining dyes. It was observed that the treatment of B16F10 cells with **5e**, **5f** and **CI994** for 48 h has shown distinct difference in cell morphology when compared to the untreated cells as evident from the Fig. 7. These observations indicate nuclear disintegration of treated cells and suggested apoptotic cell death mechanism.

#### 2.2.7. Apoptosis assay

Several reports have established that HDAC inhibitor-mediated cell death follows apoptotic pathway [54]. In order to determine the extent of apoptosis induced by the lead compounds **5e** and **5f**, Annexin-V/FITC-PI apoptotic assay was performed. B16F10 cells were treated with compounds **5e**, **5f** and **CI994** as reference compound for 72 h with the concentrations at their respective  $IC_{50}$  values. The cells were then

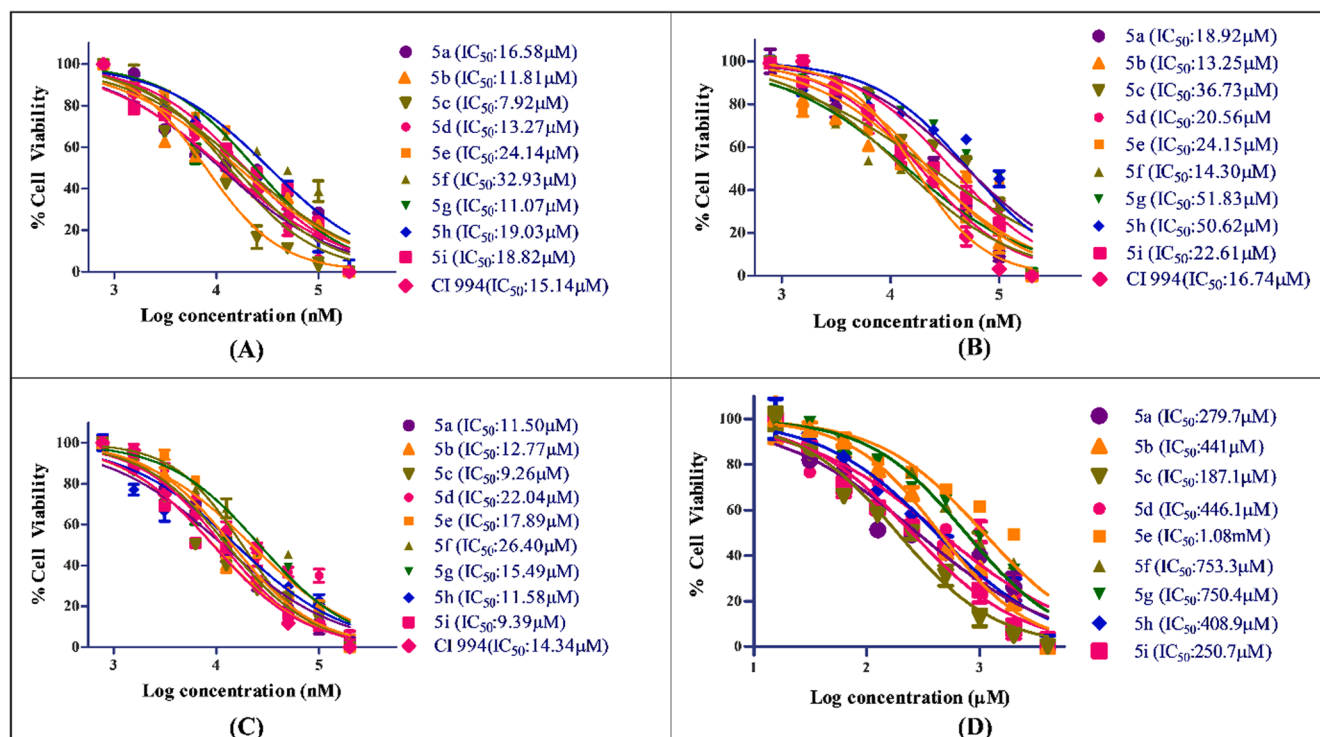


**Fig. 4.** Dose response curve and  $IC_{50}$  values of all novel compounds (**5a-5i**) along with reference molecule **CI994** as positive control on (A) MDA-MB-231, (B) 4T1, (C) B16F10 cells when treated with the compounds at concentration range of 0.7–200  $\mu\text{M}$  ( $n = 2$ ) for 72 h. Figure D represents *in vitro* cytotoxicity data on HEK293 cells when treated with the compounds at concentration range of 7–2000  $\mu\text{M}$  ( $n = 2$ ) for 72 h. Data represent mean  $\pm$  SD.  $IC_{50}$  values were calculated using nonlinear regression analysis method using Graph Pad Prism 5.

**Table 4**

The tabular presentation of  $IC_{50}$  ( $\mu\text{M}$ ) values of these novel benzamides against cancer cell lines 4T1, B16F10 and MDA-MB-231 and normal cell line HEK293 and their selectivity profile for cancer cell lines over normal cell line. Data represent mean  $\pm$  SD ( $n = 2$ ).

Compound	$IC_{50}$ ( $\mu\text{M}$ )				Selectivity for cancer cells over normal cell line		
	4T1	B16F10	MDA-MB-231	HEK293	HEK293/4T1	HEK293/B16F10	HEK293/MDA-MB-231
<b>5a</b>	18.92 $\pm$ 1.2	11.5 $\pm$ 0.98	16.58 $\pm$ 1.54	279.7 $\pm$ 8.76	14.78	24.32	16.87
<b>5b</b>	13.25 $\pm$ 0.87	12.77 $\pm$ 1.23	11.81 $\pm$ 0.87	441 $\pm$ 7.69	33.28	34.53	37.34
<b>5c</b>	36.73 $\pm$ 1.54	9.26 $\pm$ 0.69	7.92 $\pm$ 0.89	187.1 $\pm$ 4.54	5.09	20.20	23.62
<b>5d</b>	20.56 $\pm$ 1.35	22.04 $\pm$ 0.86	13.27 $\pm$ 1.68	446.1 $\pm$ 8.65	21.69	20.24	33.61
<b>5e</b>	24.15 $\pm$ 0.89	17.89 $\pm$ 1.31	24.14 $\pm$ 3.54	1084 $\pm$ 10.6	44.88	60.59	44.90
<b>5f</b>	14.30 $\pm$ 0.65	26.40 $\pm$ 2.14	32.93 $\pm$ 3.68	753.3 $\pm$ 6.8	52.67	28.53	22.87
<b>5g</b>	51.83 $\pm$ 2.35	15.49 $\pm$ 1.03	11.07 $\pm$ 1.56	750.4 $\pm$ 10.8	14.47	48.44	67.78
<b>5h</b>	50.62 $\pm$ 3.45	11.58 $\pm$ 0.78	19.03 $\pm$ 2.34	408.9 $\pm$ 2.4	8.07	35.31	21.48
<b>5i</b>	22.61 $\pm$ 1.65	9.39 $\pm$ 0.68	18.82 $\pm$ 1.98	250.7 $\pm$ 6.9	11.08	26.69	13.32
<b>CI994</b>	16.74 $\pm$ 1.65	14.34 $\pm$ 0.99	15.14 $\pm$ 1.41	216.2 $\pm$ 8.9	12.92	15.07	14.28

processed and the analysis was carried out using flow cytometry analysis. Fig. 8 displays the obtained results which suggest a significant enhanced apoptotic activity in treated cells with compounds **5e** and **5f** when compared to **CI994**. Compound **5e** displayed the total apoptotic percentage as  $20.65\% \pm 0.49$  (Q2 and Q4), whereas increased apoptotic population was observed for compound **5f** with  $35.35\% \pm 2.89$  (Q2 and Q4) when compared to **CI994** with  $16.8\% \pm 0.21$  of apoptosis. These results suggest the programmed cell death mechanism induced by compounds **5e** and **5f** leading to significant apoptosis in cancer cells.

### 2.2.8. Cell cycle analysis

In continuation to the results obtained in the apoptosis assay, the cell cycle progression was studied with the compounds **5e**, **5f** and **CI994** treatment of B16F10 cells and the cell population at different cell cycle stages was analysed using flow cytometry analysis (Fig. 9).

In the cell cycle study, B16F10 cells were treated with compounds **5e** and **5f** and reference compound **CI994** at 15  $\mu\text{M}$  concentration for 72 h.

These results (Table 5) indicated the increased cell population in G2/M phase of compound **5e** (45.14%) and compound **5f** (48.66%) when compared to control and a similar tendency was observed with **CI994** (31.74%).

The study also suggested that the cell cycle arrest at G2/M phase of the cell cycle with increased cell population containing 4n of DNA content. It was observed that compounds **5e** and **5f** showed a decrease in G1 population (31.11% and 26.28%) with no significant change in S phase (23.75% and 25.06%) when compared to reference molecule **CI994** (G1 = 43.83% and S = 24.43%). These results further emphasize the promising anticancer activity of the lead compounds (**5e** and **5f**) which might be guided through cell cycle arrest at G2/M phase. It also supports the apoptotic assay data of programmed cell death.

### 2.3. Molecular docking study

In order to understand the probable binding mode of interactions of

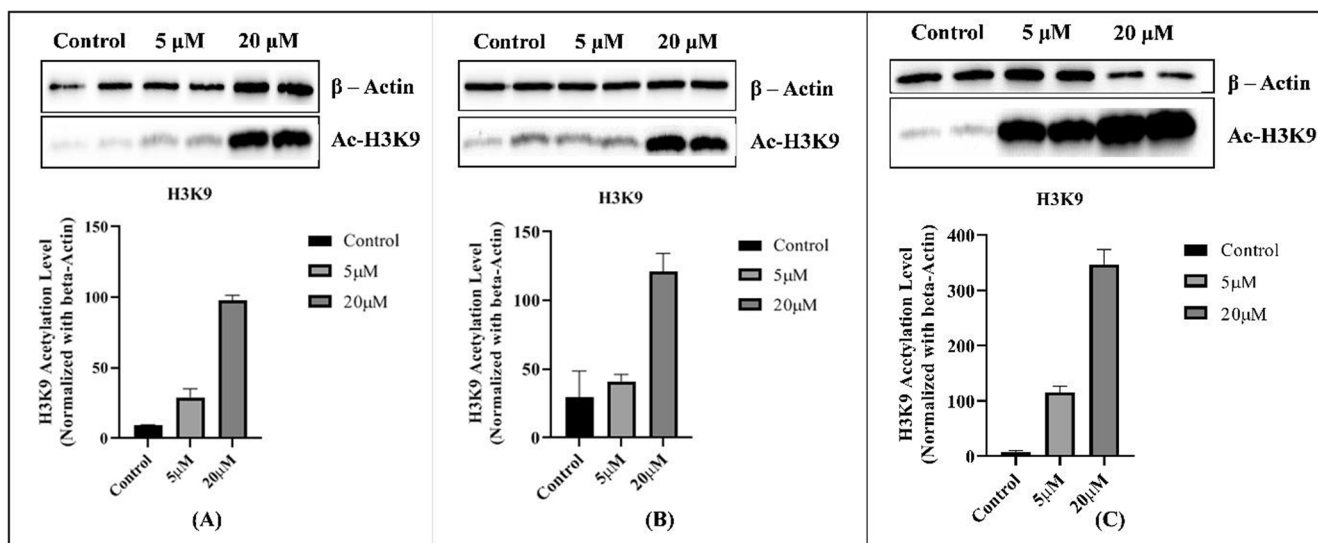


Fig. 5. Western blot of Ac-H3K9 in whole cell lysates of B16F10 murine melanoma cells after treatment with (A) compound **5e**, (B) compound **5f** and (C) **CI994** at 5  $\mu$ M and 20  $\mu$ M for 12 h. Results were normalized with respect to  $\beta$ -actin as a housekeeping control.

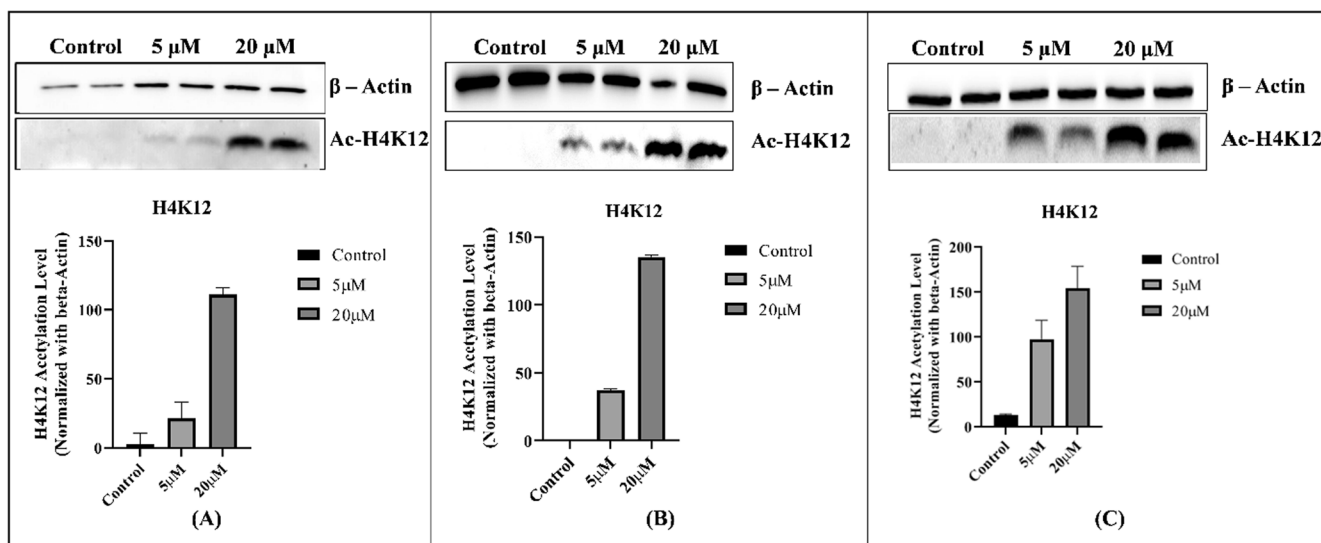


Fig. 6. Western blot of Ac-H4K12 in whole cell lysates of B16F10 murine melanoma cells after treatment with (A) compound **5e**, (B) compound **5f** and (C) **CI994** at 5  $\mu$ M and 20  $\mu$ M for 12 h. Results were normalized with respect to  $\beta$ -Actin as housekeeping control.

the promising HDAC3 inhibitors (compounds **5e** and **5f**) with HDAC3 enzyme (PDB: 4A69), molecular docking studies were performed by using Schrodinger software [55]. The docked structures of these compounds (compounds **5e** and **5f**) along with the reference molecule (**CI994**) are found to be almost superimposed with the each other on the active site of the HDAC3 as depicted in Fig. 10.

These inhibitors snugly bind to the binding groove and occupy the pocket as shown in Fig. 10. Interestingly, the docking scores are correlated with our *in vitro* HDAC3 assay results of compound **5e** (glide score:  $-6.109$ ; HDAC3  $IC_{50} = 0.560 \mu$ M), **5f** (glide score:  $-5.652$ ; HDAC3  $IC_{50} = 2.077 \mu$ M) and reference compound **CI994** (glide score:  $-5.977$ ; HDAC3  $IC_{50} = 0.902 \mu$ M).

The carbonyl group of both compounds form a hydrogen bonding interaction with Tyr298 of HDAC3 (Fig. 11).

Another hydrogen bonding interaction is noticed between the  $-NH$  function of benzamide and Gly143 of HDAC3. As seen in Fig. 11, both these inhibitors form a  $\pi$ - $\pi$  stacking interaction with Phe144. Though there are similar binding modes of interactions of these compounds, the

better HDAC3 inhibitory property of compound **5e** over compound **5f** can be explained in terms of binding mode of interactions of these compounds with HDAC3. The orientation of the 6-quinolinyl moiety (compound **5e**) at the HDAC3 active site makes it better suitable for stronger binding interaction compared to the binding orientation of 6-indolyl moiety (compound **5f**). It is important to note that the position or orientation of the heterocyclic nitrogen atom of 6-quinolinyl moiety is more or less, closer to the amide nitrogen of **CI994**. However, it is noticed that the heterocyclic nitrogen atom of 6-indolyl moiety is oriented completely opposite direction of the former ones. Therefore, 6-quinolinyl moiety is favourable than the 6-indolyl scaffold as far as the HDAC3 inhibitory potency and selectivity is concerned.

### 3. Conclusion

A series of linker-less benzamides with different aryl/heteroaryl cap moieties were designed and synthesized as promising HDAC3 inhibitors. All the compounds were studied for their *pan*-HDAC and HDAC3

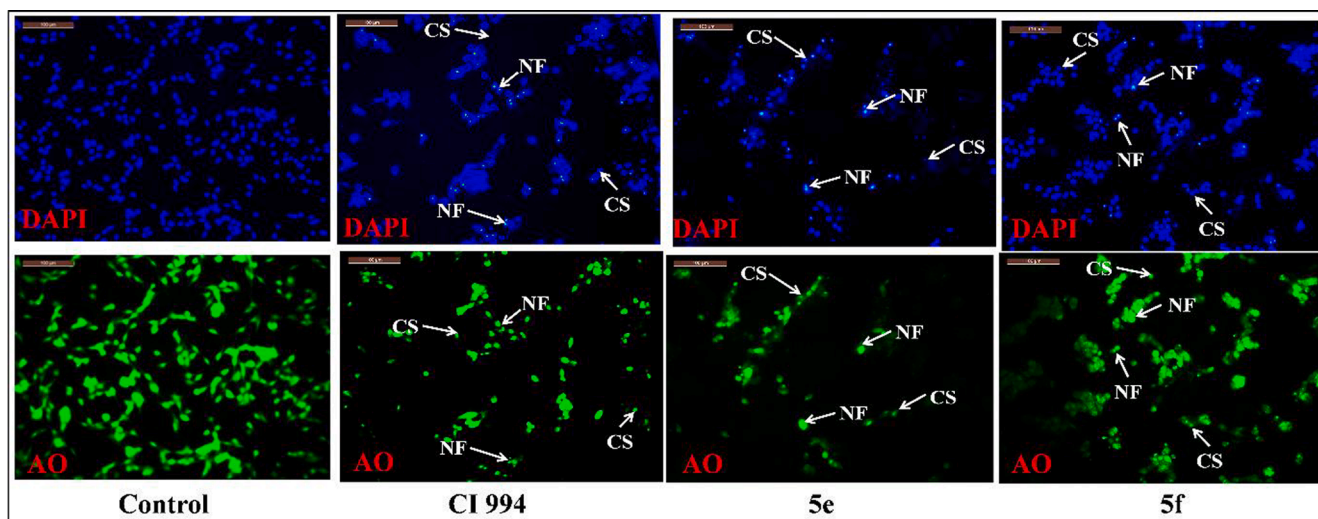


Fig. 7. Nuclear staining of B16F10 cells using DAPI (4',6-diamidino-2-phenylindole, a fluorescent stain) and acridine orange (AO) following treatment by (A) Control (B) CI994 (C) compound 5e and (D) compound 5f. The stained nuclei are visualised using fluorescence microscope (Leica microsystems, Germany) on 20x magnification.. (For interpretation of the references to colour in this figure legend, the reader is referred to the web version of this article.)

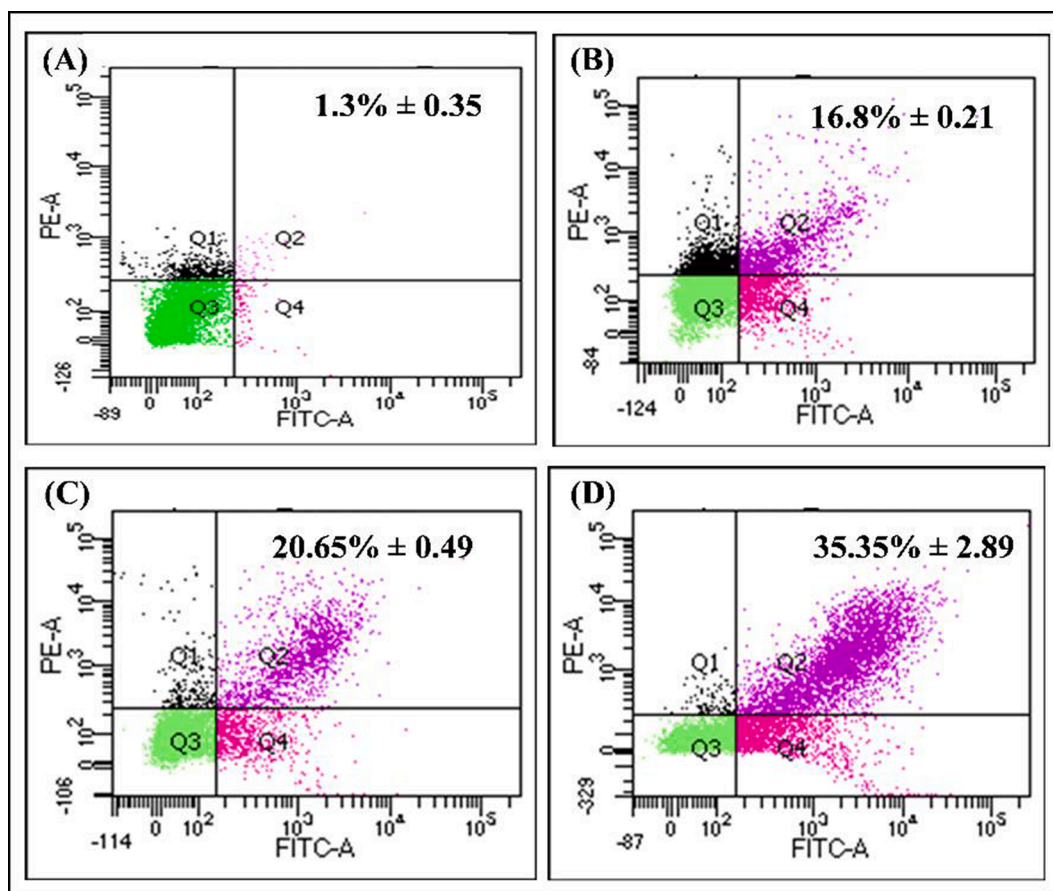


Fig. 8. Induction of apoptosis in B16F10 cells quantified by Annexin V/PI assay using flow cytometry. (A) Vehicle control (B) CI994 (C) 5e (D) 5f (Q1 – Necrotic cells, Q2 - late apoptosis, Q3 – Live cells, Q4 – early apoptotic cells, X-axis: Annexin V intensity, Y-axis: Propidium iodide intensity).

inhibitory activity. Further, the selected lead compounds 5e and 5f were studied for their HDAC 1, 2, 3, 8 and 6 enzyme inhibitory profiles to judge the selectivity towards HDAC3. Two lead compounds 5e and 5f were found to be potent and highly selective HDAC3 inhibitors over other Class-I HDACs and HDAC6. Compound 5e bearing a 6-quinolinyl moiety as the cap group was found to be a highly potent HDAC3

inhibitor ( $IC_{50} = 560$  nM) and displayed 46-fold selectivity for HDAC3 over HDAC2, and 33-fold selectivity for HDAC3 over HDAC1. Moreover, the HDAC3 selectivity of the lead molecules found to be much better than the reference compound CI994. All these compounds exhibited effective antiproliferative activity against various cancer cell lines (4T1, B16F10 and MDA-MB-231) with less cytotoxicity against normal cells

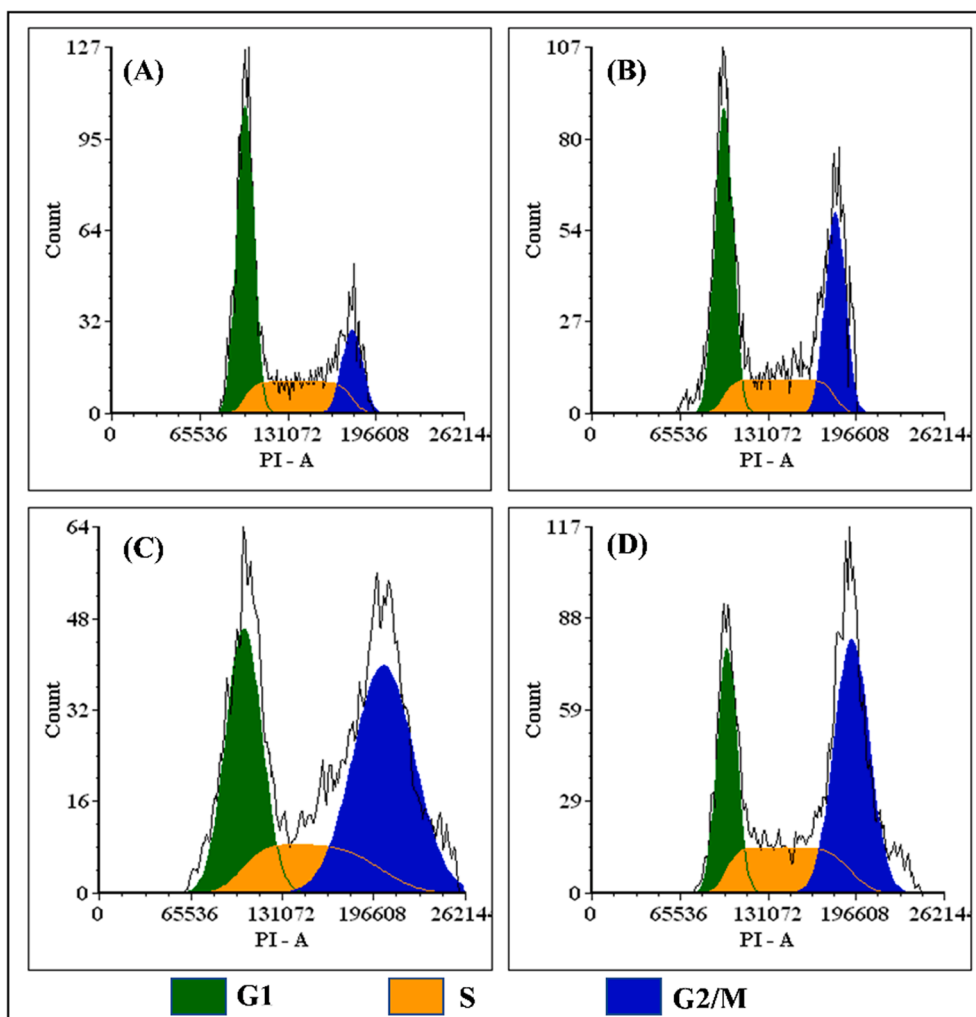


Fig. 9. Cell cycle arrest induced in murine melanoma cell B16F10 treated with (A) Control (B) CI994 as positive control (C) compound **5e** and (D) compound **5f** for 72 h. After the indicated treatment times, cell cycle analysis was performed and analysed by flow cytometry analysis (BD Aria III)®.

Table 5

The % cell population in different phases of cell cycle. Data was calculated and analysed by FCS express plus software from DNA content histograms.

Cell cycle Phase	% Cell population			
	Control	CI994	5e	5f
G1	54.27	43.83	31.11	26.28
S	28.20	24.43	23.75	25.06
G2/M	17.53	31.74	45.14	48.66

(HEK293) when compared with reference compound **CI994** and interestingly the most promising molecule (**5e**) showed least toxicity towards normal cells. Further, the acetylation levels of cellular histone (H3K9 and H4K12) were examined and both the lead compounds were able to enhance the acetylation level significantly in a dose-dependent manner in B16F10 cells. Moreover, compounds **5e** and **5f** were found to cause apoptotic cell death and were causing G2/M cell cycle phase arrest in B16F10 cells. The molecular docking study revealed similar binding interactions of the lead molecules and reference compound at the active site of HDAC3. The higher HDAC3 inhibitory potency along with selectivity for HDAC3 of compound **5e** over compound **5f** was also justified by the molecular docking analysis. Based on the findings, it can be inferred that most potent and HDAC3 selective lead molecule **5e** might serve as a potential therapeutic as anticancer agent.

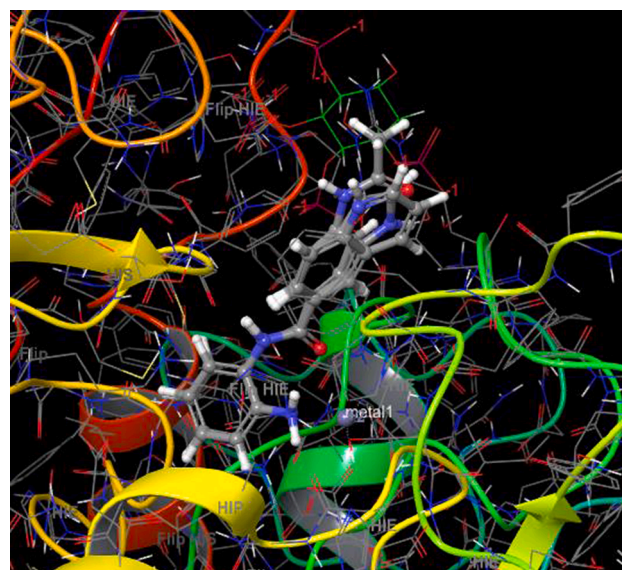


Fig. 10. The docked conformations of compounds (**5e**, **5f** and **CI994**) superimposed with each other at the active site of HDAC3 (PDB: 4A69).

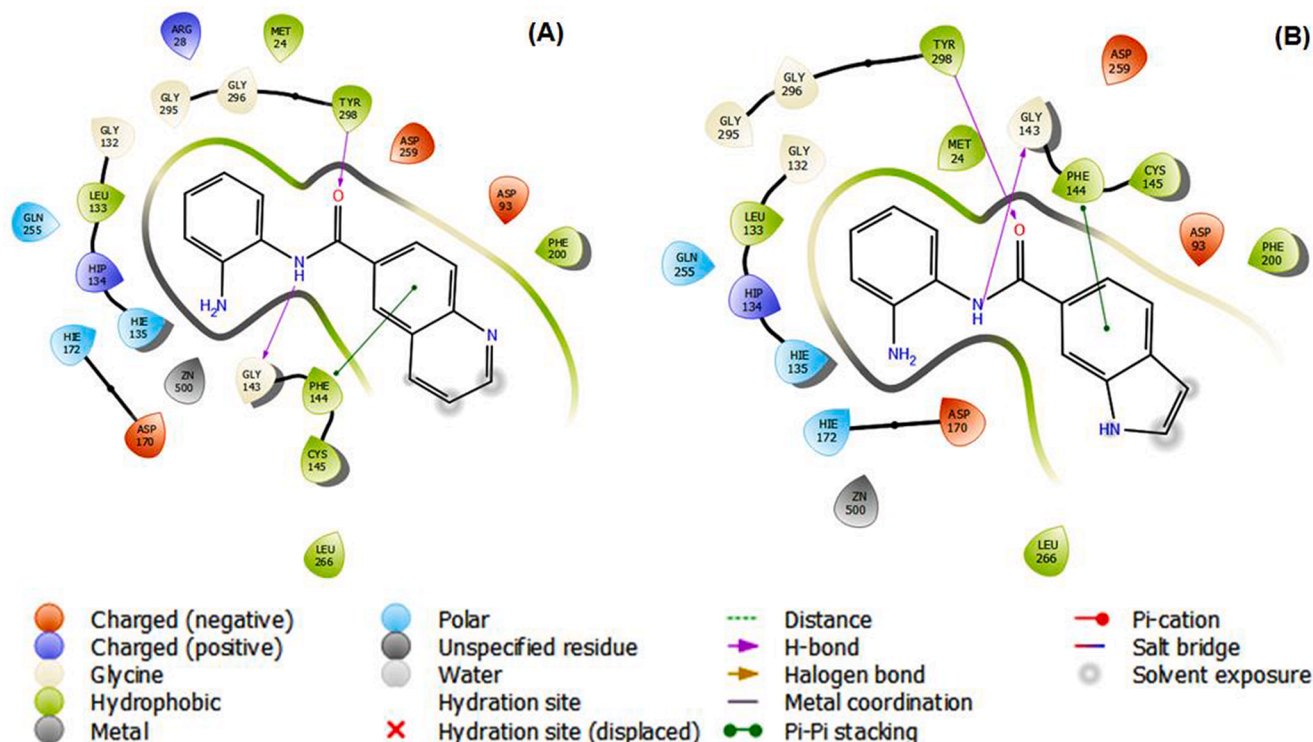


Fig. 11. Molecular docking interactions of (A) compound 5e and (B) compound 5f with HDAC3 (PDB: 4A69)

## 4. Experimental

### 4.1. General information on materials and instrumentation

All starting materials, chemicals and reagents were commercially available and were purchased from various chemical suppliers. These were used without further purification. All reactions were monitored by thin layer chromatography (TLC) using pre-coated plates with Merck 60 F254 silica gel plates purchased from Merck Millipore Co., USA and the reaction components were visualised under ultraviolet light (254 nm). Column chromatography was performed on silica gel (100 – 200 or 230 – 400 mesh size).  $^1\text{H}$  and  $^{13}\text{C}$  NMR spectrum were recorded in deuterated NMR solvents DMSO- $d_6$  and  $\text{CDCl}_3$  using Bruker, ASCEND™ 400 MHz spectrometer and the chemical shifts ( $\delta$ ) values are given in parts per million (ppm), and are internally referenced to tetramethylsilane (TMS), residual solvents peak (DMSO- $d_6$ ; 2.50 ppm  $^1\text{H}$ , 39.51 ppm  $^{13}\text{C}$ ,  $\text{CDCl}_3$ ; 7.2 ppm  $^1\text{H}$ , 77.6 ppm  $^{13}\text{C}$ ). Peak multiplicities are abbreviated as follows: s (singlet), d (doublet), t (triplet), q (quartet) and m (multiplet) while coupling constants ( $J$ ) are reported in Hz. NMR data were processed using MestReNova Software version 6.0.2–5475.

Three different cell lines were used for the determination of anticancer activity of the novel compounds synthesized. MDA-MB-231 (human breast cancer cell line), 4T1 (murine mammary carcinoma cell line), B16F10 (Murine melanoma cell line) and HEK293 (Human embryonic kidney cell line) were procured from National Centre for Cell Science (NCCS), Pune, India. B16F10, MDA-MB-231 and HEK293 cell lines were cultured in DMEM (high glucose media: AL007S, Dulbecco's modified eagle medium) and 4 T1 cell line was cultured in MEM (AT154, Minimum essential medium). All these cell lines were used for cell-culturing with 10% fetal bovine serum (FBS) and 1% antibiotic (Pen strep: A001) and were incubated at 37 °C and 5%  $\text{CO}_2$  atmosphere. Dulbecco's phosphate buffered saline (PBS), foetal bovine serum (FBS), antibiotic solution 100 × liquid with 10,000 U penicillin and 10 mg streptomycin/ml, trypsin, 3-(4,5-dimethylthiazol-2-yl)-2,5-diphenyl tetrazolium bromide (MTT) were supplied by Himedia Laboratories Pvt. Ltd., (Mumbai, India). HDAC enzyme inhibition assays were performed

as per the experimental protocol given in the enzyme kits of *pan*-HDAC (cat# BML-AK501), HDAC1 (cat# BML-AK511), HDAC2 (cat# BML-AK512), HDAC3/NCoR1 (cat# BML-AK531-0001), HDAC8 (cat# BML-AK518) from Enzo life sciences ltd. and HDAC6 (cat# K465-100) from Biovision Ltd. that were purchased from Bionova suppliers, Hyderabad. The absorbance for MTT assay and HDAC enzyme inhibition was measured using a microplate reader (Spectramax™, Molecular Devices).

### 4.2. Chemistry

All starting materials and reagents were commercially available and used without further purification. All reactions were monitored by thin layer chromatography (TLC) using pre-coated plates with silica gel F254 from Merck Millipore Co., USA.  $^1\text{H}$  and  $^{13}\text{C}$  NMR spectrum were recorded in DMSO- $d_6$  and  $\text{CDCl}_3$  using Bruker-400 MHz and chemical shifts were reported in ppm using tetramethylsilane (TMS) as internal standard. Mass spectroscopy was performed in HRMS (6545 Q-TOF LC/MS, Agilent) at Bits-Pilani, Pilani campus.

#### 4.2.1. Preparation of *tert*-butyl 2-(benzamido) phenyl carbamate (4a)

Compound (3a) (100 mg; 0.819 mmol) was dissolved in the solution of dichloromethane and pyridine (1:1) stirred at room temperature in nitrogen environment. To this reaction mixture, 1-ethyl-3-dimethyl amino propyl carbodiimide (228 mg; 1.47 mmol) and catalytic amount of 4-dimethyl amino pyridine were added. This mixture was stirred at room temperature for 20 min. After 20 min, *tert*-butyl 2-amino phenyl carbamate (187 mg; 0.90 mmol) was added into the reaction mixture and reaction was continued to 12 h. After completion of the reaction, pyridine was then evaporated under vacuum. The mixture was then dissolved in ethyl acetate and washed with sodium bicarbonate. The organic layer was then separated and dried with  $\text{Na}_2\text{SO}_4$ . The dried solvent was evaporated under vacuum. The crude product was then purified using column chromatography (solvent system – hexane and ethyl acetate (70:30)) in silica 230 – 400 mesh to obtain the final compound 4a, in its pure form (Yield 58%).  $^1\text{H}$  NMR (400 MHz,  $\text{CDCl}_3$ )  $\delta$  9.15 (s, 1H), 7.95 (d,  $J$  = 8.4 Hz, 2H), 7.76 (d,  $J$  = 7.6 Hz, 1H), 7.55 (t,  $J$

= 7.2 Hz 1H), 7.47 (t,  $J = 7.6$  Hz, 2H), 7.23 (m, 3H), 6.84 (s, 1H), 1.51 (s, 9H).  $C_{18}H_{20}N_2O_3$  [M]: 312.36; MS (ESI)  $m/z$ : [M + H]<sup>+</sup>: 313.24

#### 4.2.2. Preparation of *N*-(2-amino phenyl) benzamide (5a)

The compound *tert*-butyl-2-(benzamido) phenyl carbamate (4a) (120 mg; 0.384 mmol) was dissolved in dichloromethane (5 ml) and the solution of 4 M dioxane in HCl was added to it at 0 °C. This mixture was then allowed to react under constant stirring at room temperature for 2 h. The dioxane was then evaporated under vacuum. The resulting compound was then dissolved in ethyl acetate and washed with water. The organic layer was then separated, dried with  $Na_2SO_4$  and solvent was evaporated under vacuum. The mixture was then washed with pentane to obtain boc-protected final compound 5a. (yield: 87%). <sup>1</sup>H NMR (400 MHz,  $CDCl_3$ )  $\delta$  8.01 (s, 1H), 7.88 (d,  $J = 7.88$  Hz 2H), 7.54 (d,  $J = 7.6$  Hz 1H), 7.45 (t,  $J = 7.6$  Hz 2H), 7.28 (d,  $J = 7.6$  Hz 1H), 7.07 (t,  $J = 7.6$  Hz 1H), 6.83 (t,  $J = 5.2$  Hz 2H), 3.69 (s, 2H). <sup>13</sup>C NMR (101 MHz,  $CDCl_3$ )  $\delta$  165.87, 140.83, 134.17, 131.93, 128.75, 128.73, 127.32, 127.29, 125.39, 124.72, 119.73, 118.34.  $C_{13}H_{12}N_2O$  [M]: 212.24; MS (ESI)  $m/z$ : [M + H]<sup>+</sup>: 213.24

#### 4.2.3. Preparation of *tert*-butyl 2-(1-naphthamido) phenyl carbamate (4b)

1-Naphthoic acid (3b) (150 mg; 0.872 mmol) was dissolved in the solution of dichloromethane and pyridine (1:1) followed by the addition of 1-ethyl-3-dimethyl amino propyl carbodiimide (243.28 mg; 1.569 mmol) and catalytic amount of 4-dimethylamino pyridine. The reaction mixture was stirred at room temperature for 20 min. After 20 min, *tert*-butyl 2-amino phenyl carbamate (199 mg; 0.959 mmol) was added into the reaction mixture and reaction was continued to 12 h. The reaction mixture was monitored by TLC. After completion of the reaction, pyridine was then evaporated under vacuum. The mixture was then dissolved in ethyl acetate and washed with sodium bicarbonate. The organic layer was then separated and dried with  $Na_2SO_4$ . The dried solvent was evaporated under vacuum that was purified on a silica gel column to give compound as a solid. (yield: 74%). <sup>1</sup>H NMR (400 MHz,  $CDCl_3$ )  $\delta$  8.58 (s, 1H), 8.47 (d,  $J = 8.0$  Hz, 1H), 7.95 (d,  $J = 7.94$  Hz 1H), 7.89 (d,  $J = 8.8$  Hz 1H), 7.77 (d,  $J = 6.8$  Hz 2H), 7.57 (m, 2H), 7.48 (t,  $J = 7.6$  Hz 1H), 7.39 (d,  $J = 9.2$  Hz 1H), 7.24 (m, 2H), 6.92 (s, 1H), 1.43 (s, 9H).  $C_{22}H_{22}N_2O_3$  [M]: 361.43; MS (ESI)  $m/z$ : [M + H]<sup>+</sup>: 362.24.

#### 4.2.4. Preparation of *N*-(2-amino phenyl)-1-naphthamide (5b)

The compound *tert*-butyl-2-(1-naphthamido) phenyl carbamate (4b) (70 mg; 0.269 mmol) was dissolved in dichloromethane (5 ml). The mixture was stirred at 0 °C. To the reaction mixture solution of 4 M dioxane in HCl was added to it at same temperature. This mixture was then allowed to react under constant stirring at room temperature for 2 h. After completion of the reaction, dioxane was evaporated under vacuum. The resulting compound was quenched with water and extracted with ethyl acetate. The organic layer was then separated, dried with  $Na_2SO_4$  and solvent was evaporated under vacuum. The mixture was then washed with pentane to obtain boc-protected final compound 5b. (yield: 70%). <sup>1</sup>H NMR (400 MHz,  $DMSO-d_6$ )  $\delta$  9.84 (s, 3H), 8.33 (d,  $J = 7.6$  Hz, 1H), 8.09 (dd,  $J = 8.4, 8.8$  Hz, 2H), 7.86 (d,  $J = 6.8$  Hz, 1H), 7.62 (m, 3H), 7.38 (d,  $J = 7.6$  Hz, 1H), 7.01 (t,  $J = 7.2$  Hz, 1H), 6.84 (d,  $J = 7.6$  Hz, 1H), 6.68 (t,  $J = 7.6$  Hz, 1H), 5.05 (s, 2H). <sup>13</sup>C NMR (101 MHz,  $DMSO-d_6$ )  $\delta$ : 167.84, 142.82, 135.16, 133.64, 130.39, 128.75, 127.33, 127.10 – 126.39, 126.16, 126.16, 125.98, 125.50, 123.91, 116.84.  $C_{17}H_{14}N_2O$  [M]: 262.30; MS (ESI)  $m/z$ : [M + H]<sup>+</sup>: 263.24.

#### 4.2.5. Preparation of *tert*-butyl 2-(2-naphthamido) phenyl carbamate (4c)

To a solution of dichloromethane and pyridine (1:1) was added to 2-naphthoic acid (3c) (100 mg; 0.581 mmol) to this reaction mixture 1-ethyl-3-dimethyl amino propyl carbodiimide (243 mg; 1.56 mmol) and catalytic amount of 4-di methyl amino pyridine were added in nitrogen environment. The mixture was stirred at room temperature for 15 min. After 15 min *tert*-butyl 2-amino phenyl carbamate (216.80 mg;

0.955 mmol) was added into the reaction mixture and reaction was continued to 12 h. The reaction was monitored with TLC. After completion of the reaction, pyridine was then evaporated under vacuum. The mixture was then dissolved in sodium bicarbonate and extracted with ethylacetate. The organic layer was then separated and dried with  $Na_2SO_4$ . The dried solvent was evaporated under vacuum. The crude product was then purified using column chromatography (solvent system – hexane and ethylacetate (50:50)) in silica 230 – 400 mesh to obtain the final compound 4c in its pure form. (yield: 91%). <sup>1</sup>H NMR (400 MHz,  $CDCl_3$ )  $\delta$  9.36 (s, 2H), 8.49 (s, 1H), 8.01 (d,  $J = 10.0$  Hz, 1H), 7.93 (dd,  $J = 8, 8.8$  Hz, 3H), 7.83 (s, 1H), 7.56 (m, 2H), 7.25 (t,  $J = 4.5$  Hz, 2H), 7.16 (m, 1H), 6.99 (t,  $J = 7.6$  Hz, 1H), 6.77 (dd,  $J = 8.0, 8.4$  Hz, 1H), 1.52 (s, 9H).  $C_{22}H_{21}FN_2O_3$  [M]: 362.42; MS (ESI)  $m/z$ : [M + H]<sup>+</sup>: 363.24.

#### 4.2.6. Preparation of *N*-(2-amino phenyl)-2-naphthamide (5c)

The compound *tert*-butyl-2-(2-naphthamido) phenyl carbamate (4c) (100 mg; 0.276 mmol) was dissolved in dichloromethane (5 ml) and treated with the solution of 4 M Dioxane in HCl at 0 °C. This mixture was then allowed to react under constant stirring at room temperature for 2 h. The reaction completion was monitored by TLC. After completion of the reaction, solvent was then evaporated under vacuum. The resulting compound was then dissolved in water and extracted with ethyl acetate. The organic layer was then separated, dried with  $Na_2SO_4$  and solvent was evaporated under vacuum. The mixture was then washed with pentane to obtain boc-protected final compound 5c. (yield: 71.85%). <sup>1</sup>H NMR (400 MHz,  $DMSO-d_6$ )  $\delta$  9.86 (s, 1H), 8.64 (s, 1H), 8.05 (m, 4H), 7.63 (m, 2H), 7.26 (d,  $J = 7.6$  Hz, 1H), 7.01 (t,  $J = 8.0$  Hz, 1H), 6.84 (d,  $J = 8.0$  Hz, 1H), 6.64 (t,  $J = 6.8$  Hz, 1H), 5.04 (s, 2H). <sup>13</sup>C NMR (101 MHz,  $DMSO-d_6$ )  $\delta$  165.90, 143.65, 134.70, 132.55, 129.40, 128.60, 128.33 – 127.83, 127.51 – 126.70, 125.11, 123.85, 116.69.  $C_{17}H_{14}N_2O$  [M]: 262.30; MS (ESI)  $m/z$ : [M + H]<sup>+</sup>: 263.24.

#### 4.2.7. Preparation of *tert*-butyl 2-(quinolone-3-carboxamido) phenyl carbamate (4d)

3-Quinoline carboxylic acid (3d) (50 mg; 0.289 mmol) was dissolved in dichloromethane and pyridine (5 ml) at 0 °C. To this mixture, 1-ethyl-3-dimethylaminopropylcarbodiimide (80 mg; 0.520 mmol) and 3 mg of 4-dimethylaminopyridine were added. The mixture was allowed to react under constant stirring for 15 min before *tert*-butyl 2-amino phenyl carbamate (65.936 mg; 0.317 mmol) was added into the reaction mixture. This was allowed to react under constant stirring at room temperature for 12 h. The pyridine was then evaporated under vacuum. The mixture was then dissolved in ethyl acetate and washed with water. The organic layer was then separated and concentrated under vacuum. The crude product was then purified using column chromatography (solvent system - hexane and ethylacetate (70: 30)) in silica 60–120 mesh to obtain the final compound 4d in its pure form. (yield 76%). <sup>1</sup>H NMR (400 MHz,  $CDCl_3$ )  $\delta$  9.73 (s, 1H), 9.48 (s, 1H), 8.75 (s, 1H), 8.17 (d,  $J = 8.4$  Hz, 1H), 7.92 (m,  $J = 8.4$  Hz, 3H), 7.62 (t,  $J = 7.2$  Hz, 1H), 7.26 (m,  $J = 1.2$  Hz, 3H), 6.95 (s, 1H), 1.26 (s, 9H).  $C_{21}H_{21}N_3O_3$  [M]: 363.15; MS (ESI)  $m/z$ : [M + H]<sup>+</sup>: 364.245.

#### 4.2.8. Preparation of *N*-(2-aminophenyl) quinolone-3-carboxamide (5d)

The compound *tert*-butyl 2-(quinolone-3-carboxamido) phenyl carbamate (4d) (100 mg; 0.275 mmol) was dissolved in 5 ml DCM and 4 M dioxane HCl was added to it at 0 °C. The mixture was then allowed to react under constant stirring at room temperature for 2 h. The dioxane was then evaporated under vacuum. The mixture was then dissolved in ethylacetate and washed with water. The organic layer was then separated and concentrated under vacuum. The mixture was then washed with pentane to obtain final compound 5d. (yield 55%) <sup>1</sup>H NMR (400 MHz,  $DMSO-d_6$ )  $\delta$  10.00 (s, 1H), 9.40 (s, 1H), 9.00 (s, 1H), 8.13 (t,  $J = 8.4$  Hz 2H), 7.90 (d,  $J = 7.2$  Hz, 1H), 7.74 (s,  $J = 7.2$  Hz, 1H), 7.24 (d,  $J = 7.2$  Hz, 1H), 7.02 (s,  $J = 7.2$  Hz, 1H), 6.83 (d,  $J = 7.6$  Hz, 1H), 6.64 (s,  $J = 7.6$  Hz, 1H). <sup>13</sup>C NMR (101 MHz,  $DMSO-d_6$ )  $\delta$ :

164.5, 149.79, 149.02, 148.93, 143.20, 136.60, 131.70, 129.64, 129.25, 127.89, 127.33, 127.38, 126.99, 123.3, 116.78, 116.56, 40.19.  $C_{16}H_{13}N_3O$  [M]: 263.10; MS (ESI)  $m/z$ : [M + H]<sup>+</sup>: 264.14.

#### 4.2.9. Preparation of *tert*-butyl 2-(quinolone-6-carboxamido) phenyl carbamate (4e)

6-Quinoline carboxylic acid (3e) (100 mg; 0.578 mmol) was dissolved in dichloromethane: pyridine in the ratio of 1 : 1 (5 ml). To this mixture, 1-ethyl-3-dimethyl amino propyl carbo di imide (83.23 mg; 1.04 mmol) and 3 mg of 4-dimethylaminopyridine were added. This mixture was allowed to react under constant stirring for 15 min before *tert*-butyl 2-amino phenyl carbamate (132.08 mg; 0.635 mmol) was added into the reaction mixture. This was allowed to react under constant stirring at room temperature overnight. The pyridine was then evaporated under vacuum. The mixture was then dissolved in ethyl acetate and washed with sodium bicarbonate. The organic layer was then separated and the excess solvent was then evaporated under vacuum. The crude product was then purified using column chromatography (solvent system- hexane and ethylacetate (60:40)) in silica 230–400 mesh to obtain the final compound 4e in its pure form. (yield: 45%). <sup>1</sup>H NMR (400 MHz, CDCl<sub>3</sub>) δ 9.49 (s, 1H), 8.94 (d,  $J = 2.8$  Hz 1H), 8.44 (s, 1H), 8.18 (d,  $J = 8$  Hz 2H), 8.13 (d,  $J = 8.8$  Hz 1H), 7.82 (d,  $J = 7.6$  Hz 1H), 7.42 (dd,  $J = 4.4, 4.2$  Hz 1H), 7.14 (dd,  $J = 4.8, 4.4$  Hz 2H), 6.76 (s, 1H), 1.46 (s, 9H).  $C_{21}H_{21}N_3O_3$  [M]: 363.15; MS (ESI)  $m/z$ : [M + H]<sup>+</sup>: 364.245.

#### 4.2.10. Preparation of *N*-(2-aminophenyl) quinolone-6-carboxamide (5e)

The compound *tert*-butyl 2-(quinolone-6-carboxamido) phenyl carbamate (4e) (32 mg; 0.088 mmol) was dissolved in 5 ml DCM and 4 M dioxane HCl was added to it at 0 °C. This mixture was then allowed to react under constant stirring at room temperature for 4 h. The dioxane was then evaporated under vacuum. The mixture was then dissolved in ethylacetate and washed with sodium bicarbonate. The organic layer was then separated and the excess solvent was evaporated under vacuum. The mixture was then washed with pentane to obtain boc-deprotected final compound 5e (yield: 80%). <sup>1</sup>H NMR (400 MHz, DMSO-*d*<sub>6</sub>) δ 11.01 (s, 1H), 9.28 (s, 1H), 9.08 (s, 1H), 9.00 (d,  $J = 8$  Hz, 1H), 8.65 (d,  $J = 8.4$  Hz, 1H), 8.42 (d,  $J = 8.8$  Hz, 1H), 7.99 (dd,  $J = 4.4, 4.4$  Hz, 1H), 7.66 (d,  $J = 7.6$  Hz, 1H), 7.56 (d,  $J = 7.2$  Hz, 1H), 7.46 (dd,  $J = 7.4, 7.6$  Hz, 2H). <sup>13</sup>C NMR (101 MHz, DMSO-*d*<sub>6</sub>) δ: 165.03, 148.93, 144.78, 142.44, 133.89, 131.84, 130.19, 128.58, 128.12, 127.80, 127.33, 124.66, 123.69, 123.33 – 122.99.  $C_{16}H_{13}N_3O$  [M]: 263.10; MS (ESI)  $m/z$ : [M + H]<sup>+</sup>: 264.14.

#### 4.2.11. Preparation of *tert*-butyl 2-(1H-indole-6-carboxamido) phenyl carbamate (4f)

Indole-6-carboxylic acid (3f) (100 mg; 0.621 mmol) was dissolved in dichloromethane and added Pyridine (5 ml) under 0 °C. To this mixture, 1-ethyl-3-dimethyl amino propyl carbodiimide (107 mg, 0.690 mmol) and 5 mg of 4-dimethyl aminopyridine were added. This mixture was allowed to react under constant stirring for 15 min before *tert*-butyl 2-amino phenyl carbamate, (142.08 mg; 0.683 mmol) was added into the reaction mixture. This was allowed to react under constant stirring at room temperature overnight. Pyridine was then evaporated under vacuum. The mixture was then dissolved in ethylacetate and washed with sodium bicarbonate. The organic layer was then separated and the excess solvent was then evaporated under vacuum. The crude product was then purified using column chromatography (solvent system – hexane and ethylacetate (70:30)) in silica 60 – 120 mesh to obtain the final compound 4f in its pure form. (yield: 84%) <sup>1</sup>H NMR (400 MHz, CDCl<sub>3</sub>) δ 9.25 (s, 2H), 8.11 (s, 1H), 7.71 (d, 3H), 7.45 (dd,  $J = 3.6, 3.6$  Hz 1H), 7.33 (dd,  $J = 3.6, 3.6$  Hz 1H), 7.22 (d,  $J = 2.4$  Hz 2H), 6.61 (s, 1H), 1.57 (s, 9H).

#### 4.2.12. Preparation of *N*-(2-amino phenyl)-1H-indole-6-carboxamide (5f)

The compound *tert*-butyl –2-(1H-indole-6-carboxamido) phenyl

carbamate (4f) (140 mg; 0.398 mmol) was dissolved in 5 ml DCM and 4 M dioxane HCl was added to it at 0 °C. This mixture was then allowed to react under constant stirring at room temperature for 4 h. The dioxane was then evaporated under vacuum. The mixture was then dissolved in ethyl acetate and washed with water. The organic layer was then separated and the excess solvent was evaporated under vacuum. The mixture was then washed with pentane to obtain boc-deprotected final compound. (yield: 70%) <sup>1</sup>H NMR (400 MHz, DMSO-*d*<sub>6</sub>) δ 11.68 (s, 1H), 9.20 (s, 1H), 8.25 (s, 1H), 8.18 (d, 1H), 7.46 (dd,  $J = 3.6, 3.6$  Hz 1H), 7.13 (dd,  $J = 2.4, 3.6$  Hz 3H), 6.95 (t, 1H), 6.81 (d, 1H), 6.62 (t, 1H), 4.89 (s, 2H). <sup>13</sup>C NMR (101 MHz, DMSO-*d*<sub>6</sub>) δ: 163.74, 143.32, 136.61, 134.79, 129.11, 126.80, 126.23, 124.48, 122.46, 121.53, 120.98, 116.82, 112.34, 110.81.  $C_{15}H_{13}N_3O$  [M]: 251.10; MS (ESI)  $m/z$ : [M + H]<sup>+</sup>: 252.14.

#### 4.2.13. Preparation of *tert*-butyl 2-(1H-indole-3-carboxamido) phenyl carbamate (4g)

Indole-3-carboxylic acid (3g) (100 mg; 0.621 mmol) was dissolved in dichloromethane and added Pyridine (5 ml) under 0 °C. To this mixture, 1-ethyl-3-dimethyl amino propyl carbodiimide, (173.25 mg; 1.11 mmol) and 5 mg of 4-dimethyl aminopyridine were added. This mixture was allowed to react under constant stirring for 15 min before *tert*-butyl 2-amino phenyl carbamate (142.08 mg; 0.683 mmol) was added into the reaction mixture. This was allowed to react under constant stirring at room temperature overnight. The pyridine was then evaporated under vacuum. The mixture was then dissolved in ethylacetate and washed with sodium bicarbonate. The organic layer was then separated and the excess solvent was then evaporated under vacuum. The crude product was then purified using column chromatography (solvent system – hexane and ethylacetate (70:30)) in silica 230 – 400 mesh to obtain the final compound 4g in its pure form. (yield: 17%) <sup>1</sup>H NMR (400 MHz, DMSO-*d*<sub>6</sub>) δ 11.81 (s, 1H), 9.47 (s, 1H), 8.59 (s, 1H), 8.19 (s, 1H), 8.13 (d  $J = 7.6$  Hz, 1H), 7.57 (dd,  $J = 7.2, 7.6$  Hz, 3H), 7.15 (dd,  $J = 6.8, 6.8$  Hz 4H), 1.44 (s, 9H).  $C_{20}H_{21}N_3O_3$  [M]: 351.15; MS (ESI)  $m/z$ : [M – H]<sup>+</sup>: 350.250.

#### 4.2.14. Preparation of *N*-(2-amino phenyl)-1H-indole-3-carboxamide (5g)

The compound *tert*-butyl-2-(1H-indole-6-carboxamido) phenyl carbamate (4g) (32 mg; 0.09 mmol) was dissolved in 5 ml DCM and 4 M dioxane HCl was added to it at 0 °C. This mixture was then allowed to react under constant stirring at room temperature for 2 h. Dioxane was then evaporated under vacuum. The mixture was then dissolved in ethylacetate and washed with water. The organic layer was then separated and excess solvent was evaporated under vacuum. The mixture was then washed with pentane to obtain boc-deprotected final compound 5g. (yield: 57.3%) <sup>1</sup>H NMR (400 MHz, DMSO-*d*<sub>6</sub>) δ 11.51 (s, 1H), 9.04 (s, 1H), 8.07 (d,  $J = 7.1$  Hz, 2H), 7.29 (d,  $J = 8.0$  Hz, 1H), 7.04 (d,  $J = 3.8$  Hz, 3H), 6.78 (t,  $J = 6.4$  Hz, 1H), 6.64 (dd,  $J = 1.2, 1.2$  Hz 1H), 6.47 (dd,  $J = 1.6, 1.2$  Hz 1H), 4.72 (s, 2H). <sup>13</sup>C NMR (101 MHz, DMSO-*d*<sub>6</sub>) δ 164.09, 136.61, 128.93, 126.82, 126.37, 124.54, 122.48, 121.52, 121.00, 116.68, 112.35, 111.17 – 110.98.  $C_{15}H_{13}N_3O$  [M]: 251.105; MS (ESI)  $m/z$ : [M + H]<sup>+</sup>: 252.200.

#### 4.2.15. Preparation of *tert*-butyl 2-(thiophene-3-carboxamido) phenyl carbamate (4h)

Thiophene-3-carboxylic acid (3h) (100 mg; 0.900 mmol) was dissolved in dichloromethane and added pyridine (5 ml) at 0 °C. To this mixture, 1-ethyl-3-dimethyl amino propyl carbo di imide, (251 mg; 1.62 mmol) and 5 mg of 4-dimethylamino pyridine were added. This mixture was allowed to react under constant stirring for 15 min before *tert*-butyl 2-amino phenyl carbamate (206 mg; 0.990 mmol) was added into the reaction mixture. This was allowed to react under constant stirring at room temperature overnight. Pyridine was then evaporated under vacuum. The mixture was then dissolved in ethylacetate and washed with sodium bicarbonate. The organic layer was then separated and excess

solvent was then evaporated under vacuum. The crude product was then purified using column chromatography (solvent system – DCM and ethyl acetate (5:95)) in silica 230 – 400 mesh to obtain the final compound **4 h** in its pure form. (yield: 43%)  $^1\text{H NMR}$  (400 MHz,  $\text{CDCl}_3$ )  $\delta$  9.12 (s, 1H), 8.05 (s, 1H), 7.72 (d,  $J = 8 \text{ Hz}$  1H), 7.57 (d,  $J = 1.2 \text{ Hz}$  1H), 7.38 (dd,  $J = 2.8, 2.8 \text{ Hz}$  1H), 7.21 (dd,  $J = 1.2, 1.6 \text{ Hz}$  3H), 6.84 (s, 1H), 1.52 (s, 9H).  $\text{C}_{16}\text{H}_{20}\text{N}_2\text{O}_3\text{S}$  [M]: 318.10; MS (ESI)  $m/z$ :  $[\text{M}-\text{H}]^+$ : 317.200.

#### 4.2.16. Preparation of *N*-(2-amino phenyl)-thiophene-3-carboxamide: (5 h)

The compound *tert*-butyl-2-(thiophene-3-carboxamido) phenyl carbamate (**4 h**) (100 mg; 0.314 mmol) was dissolved in 5 ml DCM and 4 M dioxane HCl was added to it at 0 °C. This mixture was then allowed to react under constant stirring at room temperature for 2 h. Dioxane was then evaporated under vacuum. The mixture was then dissolved in ethylacetate and washed with water. The organic layer was then separated and excess solvent was evaporated under vacuum. The mixture was then washed with pentane to obtain boc-deprotected final compound **5 h**. (yield: 86%).  $^1\text{H NMR}$  (400 MHz,  $\text{DMSO}-d_6$ )  $\delta$  9.58 (s, 1H), 8.37 (s, 1H), 7.68 (d,  $J = 2.0 \text{ Hz}$  2H), 7.18 (d,  $J = 0.8 \text{ Hz}$  1H), 7.03 (t,  $J = 1.6 \text{ Hz}$  1H), 6.85 (d,  $J = 1.2 \text{ Hz}$  1H), 6.67 (t,  $J = 0.8 \text{ Hz}$  1H), 4.94 (s, 2H).  $^{13}\text{C NMR}$  (101 MHz,  $\text{DMSO}-d_6$ )  $\delta$ : 161.46, 143.96, 138.18, 129.97, 127.77, 127.260, 127.14, 127.01, 126.72, 123.49, 116.64  $\text{C}_{16}\text{H}_{18}\text{N}_2\text{O}_3\text{S}$  [M]: 318.103; MS (ESI)  $m/z$ :  $[\text{M}-\text{H}]^+$ : 317.200.  $\text{C}_{11}\text{H}_{10}\text{N}_2\text{O}_3\text{S}$  [M]: 218.05; MS (ESI)  $m/z$ :  $[\text{M} + \text{H}]^+$ : 219.1500.

#### 4.2.17. Preparation of *N*-phenyl-6-(phenyl amino) pyrazine-2-carboxamide (2i):

Aniline was added to a solution of methyl 6-chloro pyrazine-2-carboxylate (**1i**) in *N*-methylpyrrolidine at 0 °C. To the reaction mixture diisopropyl amine was added at the same temperature and the reaction was heated to 160 °C for 20 h. The completion of the reaction was monitored by TLC. Water was added to the reaction mixture and the crude compound was extracted with ethyl acetate, dried using anhydrous sodium sulphate, solvent was evaporated using rotaevaporator. The obtained crude product was purified by column chromatography.  $^1\text{H NMR}$  (400 MHz,  $\text{DMSO}-d_6$ )  $\delta$ : 10.08 (s, 1H), 9.89 (s, 1H), 8.50 (s, 1H), 8.49 (s, 1H), 7.80 (d,  $J = 9.8 \text{ Hz}$  4H), 7.47 (dd,  $J = 5.2, 12 \text{ Hz}$  4H), 7.20 (t,  $J = 8.0 \text{ Hz}$ , 1H), 7.12 (t, 6.4 Hz 1H).  $\text{C}_{17}\text{H}_{14}\text{FN}_4\text{O}$  [M]: 290.32; MS (ESI)  $m/z$ :  $[\text{M} + \text{H}]^+$ : 291.07.

#### 4.2.18. Preparation of 6-(phenyl amino) pyrazine-2-carboxylic acid (3i):

*N*-phenyl-6-(phenyl amino) pyrazine-2-carboxamide (**2i**) was dissolved in methanol and aqueous sodium hydroxide was added to the reaction mixture and the reaction was stirred at 80 °C for 1 h. The reaction was cooled at room temperature, added ice-cold water and neutralised with 1 N HCl. The compound was extracted with ethylacetate, dried using sodium sulphate and the excess solvent was evaporated using rotaevaporator. The obtained crude mixture was purified by column chromatography (solvent system – dichloromethane and methanol (7:3)).  $^1\text{H NMR}$  (400 MHz,  $\text{DMSO}-d_6$ )  $\delta$ : 9.79 (s, 1H), 8.47 (s, 2H), 7.71 (d, 2H), 7.34 (t, 2H), 7.03 (t, 1H).  $\text{C}_{11}\text{H}_9\text{FN}_3\text{O}_2$  [M]: 215.21; MS (ESI)  $m/z$ :  $[\text{M} + \text{H}]^+$ : 216.18.

#### 4.2.19. Preparation of *tert*-butyl 2-(amino phenyl)-6-phenylamino pyrazine-2-carbamate (4i):

o a solution of dichloromethane and pyridine (1:1) was added to 6-(phenyl amino) pyrazine –2-carboxylic acid (**3i**) (50 mg; 0.232 mmol). To this reaction mixture, 1-ethyl-3-dimethyl amino propyl carbo di imide (64.72 mg; 0.417 mmol) and catalytic amount of 4-dimethylamino pyridine were added in nitrogen environment. The mixture was stirred at room temperature for 15 min. After 15 min, *tert*-butyl 2-amino phenyl carbamate (53.209 mg; 0.255 mmol) was added into the reaction mixture and reaction was continued for 12 h. The reaction was monitored with TLC. After completion of the reaction, pyridine was then evaporated under vacuum. The mixture was then dissolved in sodium

bicarbonate and extracted with ethyl acetate. The organic layer was then separated and dried with  $\text{Na}_2\text{SO}_4$ . The dried solvent was evaporated under vacuum. The crude product was then purified using column chromatography (solvent system – hexane and ethylacetate (50:50)) in silica 230 – 400 mesh to obtain the final compound **4i** in its pure form. (Yield: 89%).  $^1\text{H NMR}$  (400 MHz,  $\text{CDCl}_3$ )  $\delta$   $^1\text{H NMR}$  (400 MHz,  $\text{DMSO}-d_6$ )  $\delta$  9.86 (s, 2H), 9.04 (s, 1H), 8.56 (s, 1H), 8.45 (s, 1H), 7.96 (d,  $J = 7.6 \text{ Hz}$  1H), 7.77 (d,  $J = 8 \text{ Hz}$  2H), 7.42 (t,  $J = 7.6 \text{ Hz}$  2H), 7.29 (dd,  $J = 7.6, 7.6 \text{ Hz}$  2H), 7.18 (t,  $J = 6.4 \text{ Hz}$  1H), 7.02 (t,  $J = 7.6 \text{ Hz}$  1H), 1.20 (s, 9H).  $\text{C}_{22}\text{H}_{23}\text{N}_5\text{O}_3$  [M]: 405.45; MS (ESI)  $m/z$ :  $[\text{M} + \text{H}]^+$ : 406

#### 4.2.20. Preparation of *N*-(2-aminophenyl)-6-phenylamino pyrazine-2-carboxamide (5i)

The compound *tert*-butyl 2-(amino phenyl)-6-phenylamino pyrazine-2-carbamate (**4i**) (100 mg; 0.276 mmol) was dissolved in dichloromethane (5 ml) and treated with the solution of 4 M dioxane in HCl at 0 °C. This mixture was then allowed to react under constant stirring at room temperature for 2 h. The reaction was monitored by TLC. After completion of the reaction, solvent was then evaporated under vacuum. The resulting compound was then dissolved in water and extracted with ethyl acetate. The organic layer was then separated, dried with  $\text{Na}_2\text{SO}_4$  and excess solvent was evaporated under vacuum. The mixture was then washed with pentane to obtain boc-deprotected final compound (Yield: 88.88%).  $^1\text{H NMR}$  (400 MHz,  $\text{CDCl}_3$ )  $\delta$  9.42 (s, 1H), 8.87 (s, 1H), 8.40 (s, 1H), 7.54 (d,  $J = 7.6 \text{ Hz}$  1H), 7.43 (m, 4H), 7.18 (t,  $J = 6.8 \text{ Hz}$ , 1H), 7.09 (t,  $J = 7.2 \text{ Hz}$ , 1H), 6.87 (dd,  $J = 11.5, 7.8 \text{ Hz}$ , 2H), 6.77 (s, 1H), 3.95 (s, 2H).  $^{13}\text{C NMR}$  (101 MHz,  $\text{CDCl}_3$ )  $\delta$  161.12, 150.14, 139.82, 138.40, 136.30, 134.25, 129.56, 126.88, 124.54, 124.13, 121.03, 119.95, 118.29.  $\text{C}_{17}\text{H}_{14}\text{N}_2\text{O}$  [M]: 305.33; MS (ESI)  $m/z$ :  $[\text{M} + \text{H}]^+$ : 306.

### 4.3. Biology

#### 4.3.1. Cell culture

Three different cell lines were used for the determination of anti-cancer activity of the novel compounds synthesized. For the purpose, MTT assay was carried out on Mouse breast cancer cell line (4 T1), Murine melanoma cancer cell line (B16F10) and human breast cancer (MDA-MB-231) cell line that were procured from National Centre for Cell Science (NCCS, Pune, India). B16F10 and MDA-MB-231 cell lines were cultured in DMEM (high glucose media: AL007S, Dulbecco's modified eagle medium) and 4 T1 cell line was cultured in MEM (AT154, Minimum essential medium) with 10% fetal bovine serum (FBS) and 1% antibiotic (Pen strep: A001) and were incubated at 37 °C and 5%  $\text{CO}_2$  atmosphere. MTT [3-(4,5-dimethylthiazol-2-yl)-2,5-diphenyltetrazolium bromide], a yellow dye was used for the assay. All reagents were purchased from Himedia Laboratories Pvt. Ltd., Mumbai, India.

#### 4.3.2. Chemicals and anti-bodies

All the compounds were synthesized as described above. The compounds were dissolved in DMSO stock solution and were stored in –20 °C. Primary antibodies - Rabbit mAb H3K9 acetylated histone H3 (catalogue #9649), Rabbit mAb H4K12 acetylated histone H4 (catalogue #13944), mouse mAb beta-Actin primary antibodies (catalogue #58169) and secondary antibodies – anti-rabbit HRP linked antibody and anti - mouse IgG HRP-Linked antibody were purchased from cell signalling technology. DAPI (4',6-diamidino-2- phenylindole) and acridine orange, propidium iodide and RNase were purchased from Sigma. TACs Annexin-V/FITC – PI assay kit was purchased from Biolegend and was used as per the protocol given.

#### 4.3.3. MTT assays

As per the protocol, 96 well plate was seeded with 100  $\mu\text{L}$ /well of cell suspension with the cell density of  $1 \times 10^4$  per well and were incubated for overnight. Subsequently, the medium was aspirated, and the cells were treated with the synthesized novel compounds along with **CI994** as positive control at a concentration of 100  $\mu\text{M}$  and 10  $\mu\text{M}$  in 150  $\mu\text{L}$  of

their respective media in duplicate and further incubated for 72 h. Following incubation, the culture medium was aspirated and subsequently, 50  $\mu\text{L}$  of 5 mg/ml concentrated solution of MTT (3-(4,5-dimethylthiazol-2-yl)-2,5-diphenyltetrazolium bromide) in phenol red free DMEM media was prepared and added in each well and further incubated for 3 h for the formation of formazan crystals that are formed as a result of cellular enzymatic activity. Subsequently, 150  $\mu\text{L}$  of DMSO was added to the culture after aspirating media in the wells to dissolve the formazan crystals and the absorbance was measured using multi-well plate reader Spectramax (Molecular Devices, USA) at two different wavelengths of 570 nm and 650 nm. The % cell viability was calculated as a fraction of absorbance obtained from the treated cells from the absorbance of untreated control cells. The same procedure was followed for all the three cell lines.

For the  $\text{IC}_{50}$  measurement of all the compounds in the series along with **CI994**, the same procedure was followed as described above. The DMSO solutions of the selected compounds were prepared and they were further diluted to 200  $\mu\text{M}$ , 100  $\mu\text{M}$ , 50  $\mu\text{M}$ , 25  $\mu\text{M}$ , 12.5  $\mu\text{M}$ , 6.25  $\mu\text{M}$ , 3.125  $\mu\text{M}$ , 1.562  $\mu\text{M}$  and 0.781  $\mu\text{M}$  with the DMEM complete media and MEM media respectively for the determination of  $\text{IC}_{50}$  values along with a blank control containing DMSO in medium and **CI994** as positive control and were incubated for 72 h. The experiment was repeated following the same protocol on all the 3 cell lines and the cell viability was measured by MTT assay as discussed.  $\text{IC}_{50}$  determination was also performed for the selected compounds to evaluate their cytotoxicity using Human embryonic kidney (HEK293) cell line sub-cultured in DMEM (high glucose media: AL007S, Dulbecco's modified eagle medium) with 10% fetal bovine serum (FBS) and 1% antibiotic (Pen strep: A001) and were incubated at 37  $^{\circ}\text{C}$  and 5%  $\text{CO}_2$  atmosphere. MTT [3-(4,5-dimethylthiazol-2-yl)-2,5 diphenyltetrazolium bromide], a yellow dye was used for the assay. All reagents were purchased from Himedia Laboratories Pvt. Ltd., Mumbai, India. Cytotoxicity assay was performed to study their selectivity over cancer cell lines. The DMSO solutions of the selected compounds were prepared and they were further diluted to 2 mM, 1 mM, 500  $\mu\text{M}$ , 250  $\mu\text{M}$ , 125  $\mu\text{M}$ , 62.5  $\mu\text{M}$ , 31.25  $\mu\text{M}$ , 15.62  $\mu\text{M}$  and 7.81  $\mu\text{M}$  with the DMEM complete media for the determination of  $\text{IC}_{50}$  values along with a blank control containing DMSO in medium and were incubated for 72 h.

#### 4.3.4. HDAC inhibition assays

**4.3.4.1. HDAC inhibition assay.** The enzyme inhibition assay was performed using HDAC colorimetric assay kit (BML-AK501, ENZO life sciences). Briefly, 5  $\mu\text{L}$  of HeLanuclear extract (BML-KI137-0500), 10  $\mu\text{L}$  of assay buffer (BMLKI143-0020), 10  $\mu\text{L}$  of sample solution was added per well in microtiter plate. The reaction was started with addition of 25  $\mu\text{L}$  Color de Lys<sup>®</sup> substrate solution (BML-KI138-0050). The reaction was then incubated for 30 min at 37  $^{\circ}\text{C}$ , which was terminated by addition of a 50  $\mu\text{L}$  mixture of developer (BML-KI139-0300) plus stop solution. The plate was incubated for 15 min at 37  $^{\circ}\text{C}$  and absorbance was measured at 405 nm. All synthesized compounds were screened at 10  $\mu\text{M}$  concentration in duplicate.

**4.3.4.2. HDAC1 inhibition assay.** The HDAC 1 enzyme inhibition assay was performed using HDAC 1 fluorimetric drug discovery assay kit (BML-AK511, ENZO life sciences). To the 96 well microtiter plate provided in the kit, 10  $\mu\text{L}$  of test sample solution and 15  $\mu\text{L}$  diluted HDAC1 complex solution (BML-SE456-0050) were added per well and 25  $\mu\text{L}$  Fluor de Lys<sup>®</sup> substrate solution (BML-KI177-0005) was added. The plate was incubated for 15 min at 37  $^{\circ}\text{C}$  for the reaction to occur. To terminate the reaction, 50  $\mu\text{L}$  of mixture of Fluor de Lys<sup>®</sup> developer II (BML-KI176-1250) and Trichostatin A ((BML-GR309-9090) was added per well and incubated for 45 min at 37  $^{\circ}\text{C}$  as per the protocol given in the kit. The fluorescence intensity was measured at Excitation wavelength 360 nm, Emission wavelength 460 nm using Spectramax M4

(Molecular Devices, USA). Initially, all the selected promising compounds **5e** and **5f** along with **CI994** were screened at 10  $\mu\text{M}$  concentration in duplicate. Further, all the compounds at the concentration range of 1.25  $\mu\text{M}$  – 80  $\mu\text{M}$  were tested in duplicate to find out the  $\text{IC}_{50}$  values following the same procedure as described above. The  $\text{IC}_{50}$  values of these compounds were calculated using nonlinear regression analysis method using Graph Pad Prism 5.

**4.3.4.3. HDAC2 inhibition assay.** The HDAC 2 enzyme inhibition assay was performed using HDAC 2 fluorimetric drug discovery assay kit (BML-AK512, ENZO life sciences). To the 96 well microtiter plate provided in the kit, 10  $\mu\text{L}$  of test sample solution and 15  $\mu\text{L}$  diluted HDAC2 complex solution (BML-KI575-0030) were added per well and 25  $\mu\text{L}$  Fluor de Lys<sup>®</sup> substrate solution (BML-KI572-0050) was added. The plate was incubated for 30 min at 37  $^{\circ}\text{C}$  for the reaction to occur. To terminate the reaction, 50  $\mu\text{L}$  of mixture of Fluor de Lys<sup>®</sup> developer II (BML-KI105-0300) and Trichostatin A ((BML-GR309-9090) was added per well and incubated for 15 min at 37  $^{\circ}\text{C}$  as per the protocol given in the kit. The fluorescence intensity was measured at Excitation wavelength 485 nm, Emission wavelength 530 nm using Spectramax M4 (Molecular Devices, USA). Initially, all the selected promising compounds **5e** and **5f** along with **CI994** were screened at 10  $\mu\text{M}$  concentration in duplicate. Further, all the compounds at the concentration range of 0.625  $\mu\text{M}$  – 80  $\mu\text{M}$  were tested in duplicate to find out the  $\text{IC}_{50}$  values following the same procedure as described above. The  $\text{IC}_{50}$  values of these compounds were calculated using nonlinear regression analysis method using Graph Pad Prism 5.

**4.3.4.4. HDAC3/NCOR1 inhibition assay.** The HDAC 3 enzyme inhibition assay was performed using HDAC3/NCOR1 fluorimetric drug discovery assay kit (BML-AK531-0001, ENZO life sciences). To the 96 well microtiter plate provided in the kit, 10  $\mu\text{L}$  of test sample solution and 15  $\mu\text{L}$  diluted HDAC3/NCOR1 complex solution (BMLKI574-0030) were added per well and 25  $\mu\text{L}$  Fluor de Lys<sup>®</sup> substrate solution (BML-KI177-0005) was added. The plate was incubated for 15 min at 37  $^{\circ}\text{C}$  for the reaction to occur. To terminate the reaction, 50  $\mu\text{L}$  of mixture of Fluor de Lys<sup>®</sup> developer II (BML-KI176-1250) and Trichostatin A ((BML-GR309-9090) was added per well and incubated for 45 min at 37  $^{\circ}\text{C}$  as per the protocol given in the kit. The fluorescence intensity was measured at Excitation wavelength 360 nm, Emission wavelength 460 nm using Spectramax M4 (Molecular Devices, USA). Initially, all the synthesized compounds along with **CI994** were screened at 1  $\mu\text{M}$  concentration in duplicate. The promising test compounds **5e** and **5f** along with **CI994** as positive control at the concentration range of 0.25  $\mu\text{M}$  – 8  $\mu\text{M}$  were tested in duplicate to find out the  $\text{IC}_{50}$  values following the same procedure as described above. The  $\text{IC}_{50}$  values of these compounds were calculated using nonlinear regression analysis method using Graph Pad Prism 5.

**4.3.4.5. HDAC6 inhibition assay.** The HDAC 6 enzyme inhibition assay was performed using HDAC 6 fluorimetric inhibitor screening kit (K465-100, Biovision). To the 96 well microtiter plate provided in the kit, 2  $\mu\text{L}$  of test sample solution and 50  $\mu\text{L}$  diluted HDAC2 complex solution (K465-100-2) were added per well and incubated for 15 min at 37  $^{\circ}\text{C}$ . To this 48  $\mu\text{L}$  Fluor de Lys<sup>®</sup> substrate solution (K465-100-3) was added. The plate was incubated for 30 min at 37  $^{\circ}\text{C}$  for the reaction to occur. To terminate the reaction, 10  $\mu\text{L}$  of developer II (K465-100-4) was added per well and incubated for 10 min at 37  $^{\circ}\text{C}$  as per the protocol given in the kit. The fluorescence intensity was measured at Excitation wavelength 380 nm, Emission wavelength 490 nm using Spectramax M4 (Molecular Devices, USA). Initially, all the selected promising compounds **5e**, **5f** and **CI994** were screened at 20  $\mu\text{M}$  concentration in duplicate. Further, all the compounds at the concentration range of 10  $\mu\text{M}$  – 320  $\mu\text{M}$  were tested in duplicate to find out the  $\text{IC}_{50}$  values following the same procedure as described above. The  $\text{IC}_{50}$  values of

these compounds were calculated using nonlinear regression analysis method using Graph Pad Prism 5.

**4.3.4.6. HDAC8 inhibition assay.** The HDAC 8 enzyme inhibition assay was performed using HDAC 8 fluorimetric drug discovery assay kit (BML-AK518, ENZO life sciences). To the 96 well microtiter plate provided in the kit, 10  $\mu\text{L}$  of test sample solution and 15  $\mu\text{L}$  diluted HDAC8 complex solution (BML-SE145-0100) were added per well and 25  $\mu\text{L}$  Fluor de Lys® substrate solution (BML-KI178-0005) was added. The plate was incubated for 10 min at 37 °C for the reaction to occur. To terminate the reaction, 50  $\mu\text{L}$  of mixture of Fluor de Lys® developer II (BML-KI176-1250) and Trichostatin A (BML-GR309-9090) was added per well and incubated for 45 min at 37 °C as per the protocol given in the kit. The fluorescence intensity was measured at Excitation wavelength 360 nm, Emission wavelength 460 nm using Spectramax M4 (Molecular Devices, USA). Initially, all the selected promising compounds **5e** and **5f** along with **CI994** were screened at 5  $\mu\text{M}$  concentration in duplicate. Further, all the compounds at the concentration range of 0.625  $\mu\text{M}$  – 40  $\mu\text{M}$  were tested in duplicate to find out the  $\text{IC}_{50}$  values following the same procedure as described above. The  $\text{IC}_{50}$  values of these compounds were calculated using nonlinear regression analysis method using Graph Pad Prism 5.

#### 4.3.5. Western blot analysis

For western blotting of acetylated Histone H3(H3K9) and acetylated Histone H4 (H4K12) B16F10 murine melanoma cells were plated in flat bottom 96 well plate and allow to grow overnight, and then they treated with the **5e**, **5f** and **CI994** at 5  $\mu\text{M}$ , 20  $\mu\text{M}$  final concentrations for 12 h. After the treatment, the cells were harvested by Trypsinization and centrifuge at 1250 rpm for 5 min. The cells pallet was washed by ice cold PBS, and the total protein was extracted using 100  $\mu\text{L}$ , 1X RIPA lysis buffer (Millipore, Billerica, MA, USA), supplemented with 0.5 mM phenylmethylsulfonyl fluoride (PMSF) and protease inhibitor. After lysing, the suspension was vortex and centrifuged at 14000 rpm for 15 min at 4 °C. The whole-cell lysates 20  $\mu\text{L}$  and 5  $\mu\text{L}$  of loading buffer (4X) was heated at 95 °C for 5 min and subjected to sodium dodecyl sulfate–polyacrylamide gel electrophoresis on 15% Bis-Tris 10-well gels at 60 V for approximately 180 min in SDS Running Buffer. Gels were transferred to the polyvinylidene fluoride membranes (Bio-Rad, Laboratones, Inc.) and run at 60 V for 80 min. Membranes were blocked in 5% non-fat skimmed milk (Bio-Rad, Laboratones, Inc.) in tris-buffered saline with 1% Tween 20 (TBST), and incubated with Rabbit mAb H3K9 acetylated histone H3, Rabbit mAb H4K12 acetylated histone H4 and Mouse mAb beta-Actin primary antibodies overnight at 4 °C, which were diluted up to 1:7000 in 5% (w/v) milk. The membranes were then incubated with Horseradish peroxidase (HRP)-conjugated anti-rabbit secondary antibody and anti-mouse secondary antibody and then visualized with a chemiluminescence kit (Bio-Rad, Laboratories, Inc.) and exposed using a Fusion plus 6 Imaging System (Vilber Lourmat, France). Beta-Actin was used as an internal control.

#### 4.3.6. Nuclear staining assay

The Nuclear staining were performed to investigate the status of nuclear disintegration of cancerous cells after treatment of **5e**, **5f** and **CI994** as standard by staining with DAPI (4',6-diamidino-2- phenylindole) and acridine orange. For nuclear staining, B16F10 murine melanomacells were plated in flat bottom 12 well plate and allow to grow overnight, and then they treated with the **5e** (17.89  $\mu\text{M}$ ), **5f** (26.40  $\mu\text{M}$ ) and **CI994** (14.59  $\mu\text{M}$ ) concentrations and incubate for 48 h. After 48 h of the treatment, control and compounds **5e**, **5f** and **CI994** treated group were fixed with 4% paraformaldehyde solution, thereafter both control and compounds treated cells were stained with DAPI and acridine orange. The nuclear staining of both control and treated cells was visualized under fluorescence microscope (Leica microsystems, Germany) on 20x Magnification.

#### 4.3.7. Apoptosis assay

B16F10 cells were seeded with the cell density of  $0.5 \times 10^6$ /well in 12 well tissue culture plates and left overnight. Next day cells were treated with **5e** (17.89  $\mu\text{M}$ ), **5f** (26.40  $\mu\text{M}$ ) and **CI994** (14.59  $\mu\text{M}$ ) for 72 h and the cells were incubated at 37 °C in  $\text{CO}_2$  incubator to assess the apoptosis. The study was carried out as per the manufacturer's protocol (BioLegend, US). The cells were washed with ice cold PBS, trypsinized and centrifuged to get cell pellet. The pellet was resuspended in 100  $\mu\text{L}$  reagent containing AnnexinV buffer, FITC (1  $\mu\text{L}$ ) and PI (10  $\mu\text{L}$ ) and kept for incubation for 30 min at room temperature. AnnexinV binding buffer, 1X (400  $\mu\text{L}$ ) was added to each sample and characterized by flow cytometer (BDARIA™ III). The cells with no treatment were considered as controls. FITC versus PI with quadrant gating was done as dot plot which represents (Q1 – Necrotic cells, Q2 - late apoptosis, Q3 – Live cells, Q4 – early apoptotic cells). To determine the extent of apoptosis, early and late apoptotic events were taken.

#### 4.3.8. Cell cycle analysis

The cell cycle analysis was performed by using flow cytometry. The cells B16F10 cells were seeded with density of  $0.5 \times 10^6$  cells per well. After overnight incubation, 15  $\mu\text{M}$  dose of **5e**, **5f** and **CI994** were added to cells and incubated for another 48 h. Then the cells were harvested with trypsin and the cell pellet was washed with ice cold PBS. The cells were fixed with 70% ethanol by dropwise addition into the cell suspension under gentle vortex. The clumping of cell was avoided and single cell fixation was visualized under microscope for cross-verification. The samples were kept in –20 °C for overnight. The next day fixed samples were centrifuged at 1000 rpm, 4 °C for 7 min to obtain cell pellet. Finally, the cells were re-suspended in 500  $\mu\text{L}$  of PI and RNase staining solution. The staining solution was prepared by addition of 20% w/v RNase and 2% w/v PI in 0.1% v/v of Triton X-100 solution in PBS. The samples were incubated in dark for 30 min at room temperature and analyzed by flow cytometry (BDARIA™ III). The dot plot of PI width against PI area was recorded and histogram of PI area on X axis and counts on Y axis was plotted. The percentage of cells in each phase of the cell cycle was evaluated using the FCS express software.

#### 4.4. Molecular docking

Molecular docking study was performed to predict binding interactions of promising HDAC3 inhibitors with the HDAC3 enzyme using the Glide module of Schrodinger Maestro software [55]. The protein structure (PDB: 4A69) was selected [28] and prepared by using the Glide module of Maestro software[55]. On the other hand, ligands were prepared as per our earlier mentioned protocol [28]. A grid box was created on the centroid of the HDAC3 binding site. Finally, the prepared ligands and the protein were used to execute the extra precision (XP) docking [28,56].

#### CRedit authorship contribution statement

GR, Compound synthesis and spectral analysis; SP, in vitro biological evaluation assays, Manuscript drafting and editing; TP, western blot analysis and nuclear staining assay; SAA, molecular docking studies; NA, writing the manuscript draft and designing molecular docking study, SB, validation and Supervision; TJ, validation and supervision; BG, Conceptualization, Validation, Writing- Reviewing and Supervision.

#### Declaration of competing interest

The authors declare that they have no known competing financial interests or personal relationships that could have appeared to influence the work reported in this paper.

## Acknowledgements

The research has been supported by the research fund provided by Science and Engineering Research Board-Department of Science and Technology (SERB-DST), New Delhi, India (EMR/2016/001411) and Council of Scientific and Industrial Research (CSIR-37(1722)/19/EMR-II) to Dr. Balam Ghosh, and DST-SERB, New Delhi, India to Dr. Swati Biswas (CRG/2018/001065). Sravani acknowledges CSIR for providing senior research fellowship (SRF - 09/1026(0024)/2018-EMR-I). Authors sincerely acknowledge the Department of Pharmacy, BITS-Pilani, Hyderabad, India and the Department of Pharmaceutical Technology, Jadavpur University, Kolkata, India for providing the research facilities.

## Appendix A. Supplementary data

Supplementary data to this article can be found online at <https://doi.org/10.1016/j.bioorg.2021.105050>.

## References

- <https://www.who.int/news-room/fact-sheets/detail/cancer>, (n.d.).
- S. Biswas, C.M. Rao, Epigenetics in cancer: Fundamentals and Beyond, *Pharmacology & Therapeutics*. 173 (2017) 118–134, <https://doi.org/10.1016/j.pharmthera.2017.02.011>.
- B. Sadikovic, K. Al-Romaih, J.A. Squire, M. Zielenska, Cause and consequences of genetic and epigenetic alterations in human cancer, *Curr. Genomics*. 9 (2008) 394–408, <https://doi.org/10.2174/138920208785699580>.
- S. Sharma, T.K. Kelly, P.A. Jones, Epigenetics in cancer, *Carcinogenesis*. 31 (2010) 27–36, <https://doi.org/10.1093/carcin/bgp220>.
- X.-J. Yang, E. Seto, HATs and HDACs: from structure, function and regulation to novel strategies for therapy and prevention, *Oncogene*. 26 (2007) 5310–5318, <https://doi.org/10.1038/sj.onc.1210599>.
- S. Pulya, A. Sk, N. Amin, S. Adhikari, T. Biswas, B. Ghosh Jha, HDAC6 as privileged target in drug discovery: A perspective, *Pharmacological Research*. (2020), 105274, <https://doi.org/10.1016/j.phrs.2020.105274>.
- T.R. Singh, S. Shankar, R.K. Srivastava, HDAC inhibitors enhance the apoptosis-inducing potential of TRAIL in breast carcinoma, *Oncogene*. 24 (2005) 4609–4623, <https://doi.org/10.1038/sj.onc.1208585>.
- A.J. Frew, R.W. Johnstone, J.E. Bolden, Enhancing the apoptotic and therapeutic effects of HDAC inhibitors, *Cancer Letters*. 280 (2009) 125–133, <https://doi.org/10.1016/j.canlet.2009.02.042>.
- R. Sarkar, S. Banerjee, S.A. Amin, N. Adhikari, T. Jha, Histone deacetylase 3 (HDAC3) inhibitors as anticancer agents: A review, *European Journal of Medicinal Chemistry*. 192 (2020), 112171, <https://doi.org/10.1016/j.ejmech.2020.112171>.
- Y. Li, E. Seto, HDACs and HDAC Inhibitors in Cancer Development and Therapy, *Cold Spring Harb Perspect Med*. 6 (2016), a026831, <https://doi.org/10.1101/cshperspect.a026831>.
- O. Witt, H.E. Deubzer, T. Milde, I. Oehme, HDAC family: What are the cancer relevant targets? *Cancer Letters*. 277 (2009) 8–21, <https://doi.org/10.1016/j.canlet.2008.08.016>.
- Z. Xu, Q. Tong, Z. Zhang, S. Wang, Y. Zheng, Q. Liu, L. Qian, S. Chen, J. Sun, L. Cai, Inhibition of HDAC3 prevents diabetic cardiomyopathy in OVE26 mice via epigenetic regulation of DUSP5-ERK1/2 pathway, *Clin Sci (Lond)*. 131 (2017) 1841–1857, <https://doi.org/10.1042/CS20170064>.
- S.A. Amin, N. Adhikari, S. Kotagiri, T. Jha, B. Ghosh, Histone deacetylase 3 inhibitors in learning and memory processes with special emphasis on benzamides, *Eur J Med Chem*. 166 (2019) 369–380, <https://doi.org/10.1016/j.ejmech.2019.01.077>.
- S.C. McQuown, R.M. Barrett, D.P. Matheos, R.J. Post, G.A. Rogge, T. Alenghat, S. E. Mullican, S. Jones, J.R. Rusche, M.A. Lazar, M.A. Wood, HDAC3 is a Critical Negative Regulator of Long-Term Memory Formation, *J Neurosci*. 31 (2011) 764–774, <https://doi.org/10.1523/JNEUROSCI.5052-10.2011>.
- F.H. Bardai, S.R. D’Mello, Selective Toxicity by HDAC3 in Neurons: Regulation by Akt and GSK3 $\beta$ , *J. Neurosci*. 31 (2011) 1746–1751, <https://doi.org/10.1523/JNEUROSCI.5704-10.2011>.
- C. Sathishkumar, P. Prabu, M. Balakumar, R. Lenin, D. Prabhu, R.M. Anjana, V. Mohan, M. Balasubramanyam, Augmentation of histone deacetylase 3 (HDAC3) epigenetic signature at the interface of proinflammation and insulin resistance in patients with type 2 diabetes, *Clin Epigenetics*. 8 (2016), <https://doi.org/10.1186/s13148-016-0293-3>.
- C. Angiolilli, P.A. Kabala, A.M. Grabiec, I.M.V. Baarsen, B.S. Ferguson, S. Garcia, B. M. Fernandez, T.A. McKinsey, P.P. Tak, G. Fossati, P. Mascagni, D.L. Baeten, K. A. Reedquist, Histone deacetylase 3 regulates the inflammatory gene expression programme of rheumatoid arthritis fibroblast-like synoviocytes, *Annals of the Rheumatic Diseases*. 76 (2017) 277–285, <https://doi.org/10.1136/annrheumdis-2015-209064>.
- N. Adhikari, S.A. Amin, P. Trivedi, T. Jha, B. Ghosh, HDAC3 is a potential validated target for cancer: An overview on the benzamide-based selective HDAC3 inhibitors through comparative SAR/QSAR/QAAR approaches, *Eur J Med Chem*. 157 (2018) 1127–1142, <https://doi.org/10.1016/j.ejmech.2018.08.081>.
- C.C. Spurling, C.A. Godman, E.J. Noonan, T.P. Rasmussen, D.W. Rosenberg, C. Giardina, HDAC3 overexpression and colon cancer cell proliferation and differentiation, *Molecular Carcinogenesis*. 47 (2008) 137–147, <https://doi.org/10.1002/mc.20373>.
- H.-C. Kim, K.-C. Choi, H.-K. Choi, H.-B. Kang, M.-J. Kim, Y.-H. Lee, O.-H. Lee, J. Lee, Y.-J. Kim, W. Jun, J.-W. Jeong, H.-G. Yoon, HDAC3 selectively represses CREB3-mediated transcription and migration of metastatic breast cancer cells, *Cell. Mol. Life Sci*. 67 (2010) 3499–3510, <https://doi.org/10.1007/s00018-010-0388-5>.
- J. Minami, R. Suzuki, R. Mazitschek, G. Gorgun, B. Ghosh, D. Cirstea, Y. Hu, N. Mimura, H. Ohguchi, F. Cottini, J. Jakubikova, N.C. Munshi, S.J. Haggarty, P. G. Richardson, T. Hideshima, K.C. Anderson, Histone deacetylase 3 as a novel therapeutic target in multiple myeloma, *Leukemia*. 28 (2014) 680–689, <https://doi.org/10.1038/leu.2013.231>.
- X. Shan, Y.-S. Fu, F. Aziz, X.-Q. Wang, Q. Yan, J.-W. Liu, Ginsenoside Rg3 Inhibits Melanoma Cell Proliferation through Down-Regulation of Histone Deacetylase 3 (HDAC3) and Increase of p53 Acetylation, *PLOS ONE*. 9 (2014), e115401, <https://doi.org/10.1371/journal.pone.0115401>.
- M.-H. Jeong, H. Ko, H. Jeon, G.-J. Sung, S.-Y. Park, W.J. Jun, Y.-H. Lee, J. Lee, S. Lee, H.-G. Yoon, K.-C. Choi, Delphinidin induces apoptosis via cleaved HDAC3-mediated p53 acetylation and oligomerization in prostate cancer cells, *Oncotarget*. 7 (2016) 56767–56780, <https://doi.org/10.18632/oncotarget.10790>.
- Y. Ma, Y. Yue, M. Pan, J. Sun, J. Chu, X. Lin, W. Xu, L. Feng, Y. Chen, D. Chen, V. Y. Shin, X. Wang, H. Jin, Histone deacetylase 3 inhibits new tumor suppressor gene DTWD1 in gastric cancer, *Am J Cancer Res*. 5 (2015) 663–673 (accessed September 4, 2020), <https://www.ncbi.nlm.nih.gov/pmc/articles/PMC4396045/>.
- P. Mehdipour, F. Santoro, O.A. Botrugno, M. Romanenghi, C. Pagliuca, G. M. Matthews, R.W. Johnstone, S. Minucci, HDAC3 activity is required for initiation of leukemogenesis in acute promyelocytic leukemia, *Leukemia*. 31 (2017) 995–997, <https://doi.org/10.1038/leu.2017.3>.
- R.W. Johnstone, Histone-deacetylase inhibitors: novel drugs for the treatment of cancer, *Nature Reviews Drug Discovery*. 1 (2002) 287–299, <https://doi.org/10.1038/nrd772>.
- M.G. Guenther, O. Barak, M.A. Lazar, The SMRT and N-CoR Corepressors Are Activating Cofactors for Histone Deacetylase 3, *Molecular and Cellular Biology*. 21 (2001) 6091–6101, <https://doi.org/10.1128/MCB.21.18.6091-6101.2001>.
- P.J. Watson, L. Fairall, G.M. Santos, J.W.R. Schwabe, Structure of HDAC3 bound to corepressor and inositol tetrakisphosphate, *Nature*. 481 (2012) 335–340, <https://doi.org/10.1038/nature10728>.
- P. Karagianni, J. Wong, HDAC3: taking the SMRT-N-CoR road to repression, *Oncogene*. 26 (2007) 5439–5449, <https://doi.org/10.1038/sj.onc.1210612>.
- P.M. Lombardi, K.E. Cole, D.P. Dowling, D.W. Christianson, Structure, Mechanism, and Inhibition of Histone Deacetylases and Related Metalloenzymes, *Curr Opin Struct Biol*. 21 (2011) 735–743, <https://doi.org/10.1016/j.sbi.2011.08.004>.
- M. Dokmanovic, C. Clarke, P.A. Marks, Histone Deacetylase Inhibitors: Overview and Perspectives, *Mol Cancer Res*. 5 (2007) 981–989, <https://doi.org/10.1158/1541-7786.MCR-07-0324>.
- X. Lu, Z. Ning, Z. Li, H. Cao, X. Wang, Development of chidamide for peripheral T-cell lymphoma, the first orphan drug approved in China, *Intractable Rare Dis Res*. 5 (2016) 185–191, <https://doi.org/10.5582/irdr.2016.01024>.
- J. Knipstein, L. Gore, Entinostat for treatment of solid tumors and hematologic malignancies, *Expert Opinion on Investigational Drugs*. 20 (2011) 1455–1467, <https://doi.org/10.1517/13543784.2011.613822>.
- Z.-Y. Li, Q.-Z. Li, L. Chen, B.-D. Chen, B. Wang, X.-J. Zhang, W.-P. Li, Histone Deacetylase Inhibitor RGFP109 Overcomes Temozolomide Resistance by Blocking NF- $\kappa$ B-Dependent Transcription in Glioblastoma Cell Lines, *Neurochem. Res*. 41 (2016) 3192–3205, <https://doi.org/10.1007/s11064-016-2043-5>.
- M. Loprevite, M. Tiseo, F. Grossi, T. Scolaro, C. Semino, A. Pandolfi, R. Favoni, A. Ardizzone, In Vitro Study of CI-994, a Histone Deacetylase Inhibitor, Non-Small Cell Lung Cancer Cell Lines, *Oncology Research Featuring Preclinical and Clinical Cancer Therapeutics*. 15 (2005) 39–48, <https://doi.org/10.3727/096504005775082066>.
- S. Prakash, B.J. Foster, M. Meyer, A. Wozniak, L.K. Heilbrun, L. Flaherty, M. Zalupski, L. Radulovic, M. Valdiviosio, P.M. LoRusso, Chronic Oral Administration of CI-994: A Phase I Study, *Invest New Drugs*. 19 (2001) 1–11, <https://doi.org/10.1023/A:1006489328324>.
- T. Beckers, C. Burkhardt, H. Wieland, P. Gimnich, T. Ciossek, T. Maier, K. Sanders, Distinct pharmacological properties of second generation HDAC inhibitors with the benzamide or hydroxamate head group, *International Journal of Cancer*. 121 (2007) 1138–1148, <https://doi.org/10.1002/ijc.22751>.
- F.F. Wagner, M. Lundh, T. Kaya, P. McCarren, Y.-L. Zhang, S. Chattopadhyay, J. P. Gale, T. Galbo, S.L. Fisher, B.C. Meier, A. Vetere, S. Richardson, N.G. Morgan, D. P. Christensen, T.J. Gilbert, J.M. Hooker, M. Leroy, D. Walpita, T. Mandrup-Poulsen, B.K. Wagner, E.B. Holson, An Isochemogenic Set of Inhibitors To Define the Therapeutic Potential of Histone Deacetylases in  $\beta$ -Cell Protection, *ACS Chem. Biol*. 11 (2016) 363–374, <https://doi.org/10.1021/acschembio.5b00640>.
- Y. Chen, R. He, Y. Chen, M.A. D’Annibale, B. Langley, A.P. Kozikowski, Studies of Benzamide- and Thiol-Based Histone Deacetylase Inhibitors in Models of Oxidative-Stress-Induced Neuronal Death: Identification of Some HDAC3-Selective Inhibitors, *ChemMedChem*. 4 (2009) 842–852, <https://doi.org/10.1002/cmdc.200800461>.
- R. He, Y. Chen, Y. Chen, A.V. Ougolkov, J.-S. Zhang, D.N. Savoy, D.D. Billadeau, A. P. Kozikowski, Synthesis and Biological Evaluation of Triazol-4-ylphenyl-Bearing Histone Deacetylase Inhibitors as Anticancer Agents, *J. Med. Chem*. 53 (2010) 1347–1356, <https://doi.org/10.1021/jm901667k>.
- M. Boissinot, M. Inman, A. Hempshall, S.R. James, J.H. Gill, P. Selby, D.T. Bowen, R. Grigg, P.N. Cockerill, Induction of differentiation and apoptosis in leukaemic

- cell lines by the novel benzamide family histone deacetylase 2 and 3 inhibitor MI-192, *Leukemia Research*. 36 (2012) 1304–1310, <https://doi.org/10.1016/j.leukres.2012.07.002>.
- [42] T. Suzuki, Y. Kasuya, Y. Itoh, Y. Ota, P. Zhan, K. Asamitsu, H. Nakagawa, T. Okamoto, N. Miyata, Identification of Highly Selective and Potent Histone Deacetylase 3 Inhibitors Using Click Chemistry-Based Combinatorial Fragment Assembly, *PLOS ONE*. 8 (2013), e68669, <https://doi.org/10.1371/journal.pone.0068669>.
- [43] C.M. Marson, C.J. Matthews, E. Yiannaki, S.J. Atkinson, P.E. Soden, L. Shukla, N. Lamadema, N.S.B. Thomas, Discovery of Potent, Isoform-Selective Inhibitors of Histone Deacetylase Containing Chiral Heterocyclic Capping Groups and a N-(2-Aminophenyl)benzamide Binding Unit, *J. Med. Chem.* 56 (2013) 6156–6174, <https://doi.org/10.1021/jm400634n>.
- [44] C.M. Marson, C.J. Matthews, S.J. Atkinson, N. Lamadema, N.S.B. Thomas, Potent and Selective Inhibitors of Histone Deacetylase-3 Containing Chiral Oxazoline Capping Groups and a N-(2-Aminophenyl)-benzamide Binding Unit, *J. Med. Chem.* 58 (2015) 6803–6818, <https://doi.org/10.1021/acs.jmedchem.5b00545>.
- [45] X. Li, Y. Zhang, Y. Jiang, J. Wu, E.S. Inks, C.J. Chou, S. Gao, J. Hou, Q. Ding, J. Li, X. Wang, Y. Huang, W. Xu, Selective HDAC inhibitors with potent oral activity against leukemia and colorectal cancer: Design, structure-activity relationship and anti-tumor activity study, *European Journal of Medicinal Chemistry*. 134 (2017) 185–206, <https://doi.org/10.1016/j.ejmech.2017.03.069>.
- [46] H.-Y. Hsieh, H.-C. Chuang, F.-H. Shen, K. Detroja, L.-W. Hsin, C.-S. Chen, Targeting breast cancer stem cells by novel HDAC3-selective inhibitors, *European Journal of Medicinal Chemistry*. 140 (2017) 42–51, <https://doi.org/10.1016/j.ejmech.2017.08.069>.
- [47] J. Zang, X. Liang, Y. Huang, Y. Jia, X. Li, W. Xu, C.J. Chou, Y. Zhang, Discovery of Novel Pazopanib-Based HDAC and VEGFR Dual Inhibitors Targeting Cancer Epigenetics and Angiogenesis Simultaneously, *J. Med. Chem.* 61 (2018) 5304–5322, <https://doi.org/10.1021/acs.jmedchem.8b00384>.
- [48] J.J. McClure, E.S. Inks, C. Zhang, Y.K. Peterson, J. Li, K. Chundru, B. Lee, A. Buchanan, S. Miao, C.J. Chou, Comparison of the Deacetylase and Deacetylase Activity of Zinc-Dependent HDACs, *ACS Chem. Biol.* 12 (2017) 1644–1655, <https://doi.org/10.1021/acschembio.7b00321>.
- [49] P. Trivedi, N. Adhikari, A. Sk, T. Amin, B. Ghosh Jha, Design, synthesis and biological screening of 2-aminobenzamides as selective HDAC3 inhibitors with promising anticancer effects, *European Journal of Pharmaceutical Sciences*. 124 (2018) 165–181, <https://doi.org/10.1016/j.ejps.2018.08.030>.
- [50] P. Trivedi, N. Adhikari, A. Sk, Y. Amin, R. Bobde, T. Ganesh, B. Ghosh Jha, Design, synthesis, biological evaluation and molecular docking study of arylcarboxamido piperidine and piperazine-based hydroxamates as potential HDAC3 inhibitors with promising anticancer activity, *European Journal of Pharmaceutical Sciences*. 138 (2019), 105046, <https://doi.org/10.1016/j.ejps.2019.105046>.
- [51] S.A. Amin, N. Adhikari, T. Jha, B. Ghosh, Designing potential HDAC3 inhibitors to improve memory and learning, *Journal of Biomolecular Structure and Dynamics*. 37 (2019) 2133–2142, <https://doi.org/10.1080/07391102.2018.1477625>.
- [52] M.M.S. Hamoud, S. Pulya, N.A. Osman, Y. Bobde, A.E.A. Hassan, H.A. Abdel-Fattah, B. Ghosh, A.M. Ghanim, Design, synthesis, and biological evaluation of novel nicotinamide derivatives as potential histone deacetylase-3 inhibitors, *New J. Chem.* (2020), <https://doi.org/10.1039/D0NJ01274B>.
- [53] S. Pulya, A. Mahale, Y. Bobde, G. Routholla, T. Patel, S. Swati, V. Biswas, O. P. Sharma, B. Ghosh Kulkarni, PT3: A Novel Benzamide Class Histone Deacetylase 3 Inhibitor Improves Learning and Memory in Novel Object Recognition Mouse Model, *ACS Chem. Neurosci.* (2021), <https://doi.org/10.1021/acschemneuro.0c00721>.
- [54] J. Zhang, Q. Zhong, Histone deacetylase inhibitors and cell death, *Cell Mol Life Sci*. 71 (2014) 3885–3901, <https://doi.org/10.1007/s00018-014-1656-6>.
- [55] Schrödinger Suite, Schrödinger, LLC, New York, USA, 2019. <http://www.schrodinger.com/glide>, n.d.
- [56] S.K. Baidya, A. Sk, S. Amin, N. Banerjee, T.Jh.a. Adhikari, Structural exploration of arylsulfonamide-based ADAM17 inhibitors through validated comparative multi-QSAR modelling studies, *Journal of Molecular Structure*. 1185 (2019) 128–142, <https://doi.org/10.1016/j.molstruc.2019.02.081>.